Published OnlineFirst May 12, 2011; DOI:10.1158/0008-5472.CAN-10-2475

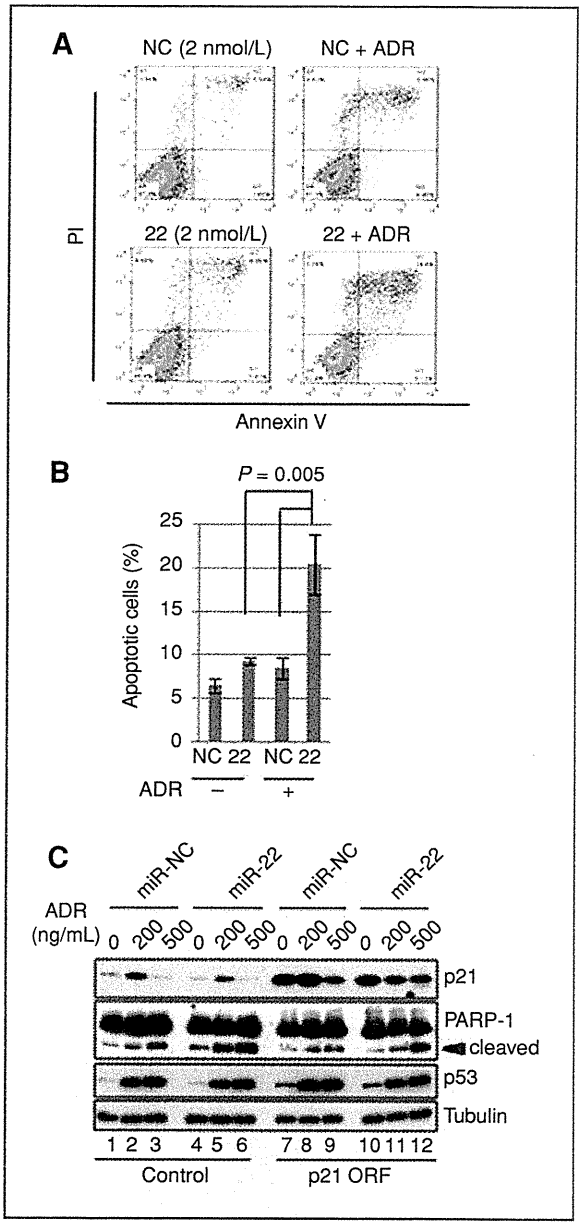

Figure 5. A, sensitization to p53-dependent apoptosis by *miR-22*. HCT 116 cells, transfected with either 2 nmol/L of *miR-22* or miR-NC, were incubated in the presence or absence of 100 ng/mL ADR for 12 hours. Apoptotic cells were determined by FACS. B, quantification of apoptotic cells using 3 independent FACS experiments as described in (A). Data show mean with SD. C, expression of p21 protein reduced *miR-22*-induced sensitization of apoptosis. HCT 116 cells were transduced with either control or *p21* ORF lentivirus. After selection, cells transfected with either miR-NC or *miR-22* were treated with indicated concentration of ADR for 24 hours and cleaved PARP-1 was detected by immunoblotting.

and its role in the determination of p53-dependent cellular fate through the formation of the p53–*miR-22*–p21 axis was shown. This axis might be activated by specific stresses that require the elimination of damaged cells. The current findings provide a novel insight into the regulatory mechanism of cell fate determination by a specific molecule, *miR-22*, in response to various oncogenic stresses and in a p53-dependent manner.

As depicted in Fig. 6E, 2 modes of action of the p53–*miR-22*–p21 axis were suggested in response to the different intensity of the stresses applied. In brief, p53 only activates p21 to induce cell-cycle arrest against weak stresses in the p53–p21 pathway. On the other hand, severe damage transcriptionally activates both *p21* and *miR-22*, and *miR-22* represses p21 expression through the inhibition of protein synthesis and enhancement of p21 mRNA degradation. Under severe damage conditions, apoptosis may be induced by entry into the cell cycle via direct repression of p21 by *miR-22*.

Antiapoptotic function of p21 has recently attracted attention for its oncogenic action, which is opposed to a traditional tumor suppressor function. Lack of *p21* induces apoptosis through the accumulation of DNA damage in leukemic stem cells (41). Disruption of the *p21* gene sensitized cancer cells to apoptosis after treatment with chemotherapeutic agents (37, 38). Recently, the small molecule RITA, an activator of p53, was shown to efficiently induce apoptosis through inhibition of p21 (42). Furthermore, a single recombinant adenovirus containing *p53* cDNA and synthetic *p21* shRNA also efficiently induced apoptosis in colon cancer cell lines (43). These findings indicate that the downregulation or inhibition of p21 after activation of p53 in stressed cells is one of the key factors as an anticancer mechanism by inducing the change of cellular phenotype from cell-cycle arrest to apoptosis, which could be the mechanism triggered by *miR-22* as an intrinsic stress–response network.

MicroRNAs are known to repress multiple target mRNAs, leading to efficient shut down or activation of intracellular networks (44, 45). Indeed, introduction of *miR-22* broadly and significantly modulates cellular networks in p53 wild-type HCT 116 cells (Supplementary Tables S3, S4, and Fig. S3D). Furthermore, high levels of expression of *miR-22* alone clearly showed apoptosis without activation of p53 in HCT 116 cells (Fig. 2A), where p21 might not be a promising target of *miR-22*, suggesting that other *miR-22* target genes also contribute to the induction of p53-dependent apoptosis.

In addition to the *miR-22* function in p53 wild-type colon cancer cells, another interesting feature is that *miR-22* expression induces cell-cycle arrest in p53 knockout and mutant cell lines (Supplementary Fig. S3B and C). We searched for a TargetScan database to obtain a list of potential *miR-22* targets and conducted gene ontology analysis to identify genes whose repression theoretically induces cell-cycle arrest. These analyses indicated that several positive cell-cycle regulators, *CDK6*, *CDK3*, *SIRT1*, *CDC25B*, and *HDAC4*, are possible targets of *miR-22*. We analyzed the protein levels of CDK6 and SIRT1 by immunoblot analysis, and found no significant changes in their protein levels in the presence of *miR-22* in SW480 cells. Then, we re-evaluated the data of AGO2-IP on ChIP analysis using HCT 116 cells. Interestingly, *CDK3*, *CDC25B*, and *HDAC4* mRNAs were enriched in the AGO2 complex in a *miR-22*-dependent manner (data not shown). Although it is currently unclear that these mRNAs are directly

Published OnlineFirst May 12, 2011; DOI:10.1158/0008-5472.CAN-10-2475

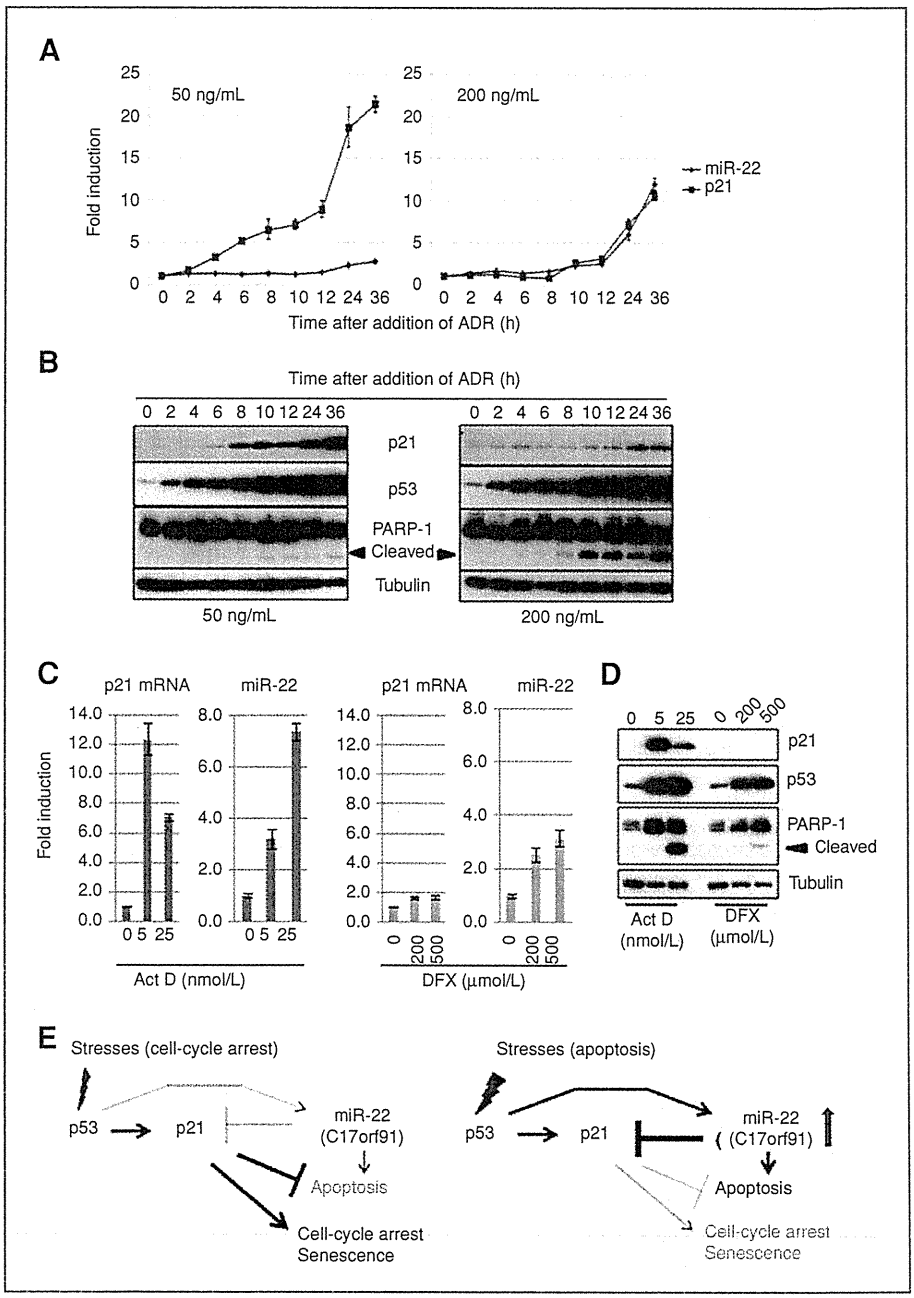

Figure 6. A and B, kinetics of *miR-22* and p21 increments after exposure to ADR. Time-dependent increments of *p21* mRNA and *miR-22* after exposure to different doses of ADR were quantified by RT-PCR. Relative expression of *p21* and *miR-22* was calculated by $2^{-\Delta\Delta ct}$ using *GAPDH* as an internal standard (A). Protein levels of p21, p53, and cleaved PARP-1 were analyzed by immunoblotting in cells treated with different doses of ADR (B). C and D, activation of *miR-22* expression by Act D. Cells were treated with specific concentration of either Act D or deferoxiamine for 24 hours, and p21 and *miR-22* levels were determined as described above. E, 2 modes of action of *miR-22* in the p53 network.

downregulated by *miR-22*, *miR-22* may induce p53 independent cell-cycle arrest through the repression of these genes.

The present data suggest a tumor-suppressive role of *miR-22* in colon cancer cells. *MiR-22* was also reported to be downregulated in estrogen receptor (ER)-positive breast cancers, and repression of ER expression by *miR-22* suppressed cell proliferation (46, 47). On the other hand, *miR-22* was recently suggested to have an oncogenic role through the direct silencing of *PTEN* and its upregulation in prostate cancer cell lines (48). These authors identified the transforming activity of *miR-22* in mouse embryonic fibroblast cooperatively with *c-Myc*, and showed that the overexpression of *miR-22* in the prostate cancer cell line DU145, harboring p53 mutations in both alleles, caused an enhancement of colony formation. The reported paradoxical function of *miR-22* implies that *miR-22* could act as a tissue-specific or context-dependent tumor suppressor gene.

Chromosome 17p13.3, where the *miR-22* gene resides, is well known to be a target for allelic loss, and loss of heterozygosity in 17p13.3 is often found independently of

Published OnlineFirst May 12, 2011; DOI:10.1158/0008-5472.CAN-10-2475

the *TP53* mutation in human cancers, including lung and breast cancer (49, 50). Furthermore, an unknown tumor suppressor gene has been suggested to be present at this locus. The present data suggest that *miR-22* is a candidate haploinsufficient-type tumor suppressor gene within this region, and its hemizygous loss or downregulation reduced apoptosis induction in response to stresses, even in cells retaining an intact *TP53*.

In summary, the data presented suggest a role for *miR-22* as an intrinsic molecular switch in the p53 tumor suppressor network, functioning as a determinant of cell fate at a post-transcriptional level by inducing apoptosis via direct repression of *p21*. This system might function in the p53-dependent activation of a specific anticancer barrier in response to various oncogenic stresses, and dysfunction of *miR-22* might confer a chance of survival for damaged cells with tumorigenic potential.

Disclosure of Potential Conflicts of Interest

No potential conflicts of interest were disclosed.

Acknowledgments

We would like to thank Drs. Hirofumi Arakawa, Masato Enari, Hiroki Sasaki, Kazuhiko Aoyagi, and Ryo-u Takahashi at NCCRI for providing us with antibodies, the p21 expression vector, bioinformatics analysis, technical support, and helpful discussions.

Grant Support

This work is supported by the Program for Promotion of Fundamental Studies in Health Sciences of the National Institute of Biomedical Innovation (NIBIO), a Grant-in-Aid for 3rd Term Comprehensive 10-Year Strategy for Cancer Control from the Ministry of Health, Labor and Welfare, Japan, a grant from Takeda Science Foundation (H. Nakagama), and a Grant-in-Aid for Scientific Research from the Ministry of Education, Culture, Sports & Technology of Japan (N. Tsuchiya). H. Ogata-Kawata is an awardee of the Research Resident Fellowship from the Foundation for Promotion of Cancer Research Japan for the 3rd Term Comprehensive 10-Year Strategy for Cancer Control.

The costs of publication of this article were defrayed in part by the payment of page charges. This article must therefore be hereby marked *advertisement* in accordance with 18 U.S.C. Section 1734 solely to indicate this fact.

Received July 8, 2010; revised May 9, 2011; accepted May 9, 2011; published OnlineFirst May 12, 2011.

References

1. Levine AJ. p53, the cellular gatekeeper for growth and division. Cell 1997;88:323–31.
2. Vousden KH, Prives C. Blinded by the light: the growing complexity of p53. Cell 2009;137:413–31.
3. Beausejour CM, Krtolica A, Galimi F, Narita M, Lowe SW, Yaswen P, et al. Reversal of human cellular senescence: roles of the p53 and p16 pathways. EMBO J 2003;22:4212–22.
4. Harris SL, Levine AJ. The p53 pathway: positive and negative feedback loops. Oncogene 2005;24:2899–908.
5. Oda E, Ohki R, Murasawa H, Nemoto J, Shibue T, Yamashita T, et al. Noxa, a BH3-only member of the Bcl-2 family and candidate mediator of p53-induced apoptosis. Science 2000;288:1053–8.
6. Yu J, Zhang L, Hwang PM, Kinzler KW, Vogelstein B. PUMA induces the rapid apoptosis of colorectal cancer cells. Mol Cell 2001;7:673–82.
7. Miyashita T, Reed JC. Tumor suppressor p53 is a direct transcriptional activator of the human bax gene. Cell 1995;80:293–9.
8. Ashcroft M, Taya Y, Vousden KH. Stress signals utilize multiple pathways to stabilize p53. Mol Cell Biol 2000;20:3224–33.
9. Kruse JP, Gu W. Modes of p53 regulation. Cell 2009;137:609–22.
10. D'Orazi G, Cecchinelli B, Bruno T, Manni I, Higashimoto Y, Saito S, et al. Homeodomain-interacting protein kinase-2 phosphorylates p53 at Ser 46 and mediates apoptosis. Nat Cell Biol 2002;4:11–9.
11. Oda K, Arakawa H, Tanaka T, Matsuda K, Tanikawa C, Mori T, et al. p53AIP1, a potential mediator of p53-dependent apoptosis, and its regulation by Ser-46-phosphorylated p53. Cell 2000;102:849–62.
12. Tang Y, Luo J, Zhang W, Gu W. Tip60-dependent acetylation of p53 modulates the decision between cell-cycle arrest and apoptosis. Mol Cell 2006;24:827–39.
13. Ambros V, Lee RC, Lavanway A, Williams PT, Jewell D. MicroRNAs and other tiny endogenous RNAs in C. elegans. Curr Biol 2003;13:807–18.
14. Plasterk RH. Micro RNAs in animal development. Cell 2006;124:877–81.
15. Stefani G, Slack FJ. Small non-coding RNAs in animal development. Nat Rev Mol Cell Biol 2008;9:219–30.
16. Voorhoeve PM, Agami R. Classifying microRNAs in cancer: the good, the bad and the ugly. Biochim Biophys Acta 2007;1775:274–82.
17. Croce CM. Causes and consequences of microRNA dysregulation in cancer. Nat Rev Genet 2009;10:704–14.
18. Schetter AJ, Leung SY, Sohn JJ, Zanetti KA, Bowman ED, Yanaihara N, et al. MicroRNA expression profiles associated with prognosis and therapeutic outcome in colon adenocarcinoma. JAMA 2008;299:425–36.
19. He L, Thomson JM, Hemann MT, Hernando-Monge E, Mu D, Goodson S, et al. A microRNA polycistron as a potential human oncogene. Nature 2005;435:828–33.
20. Lu J, Getz G, Miska EA, Alvarez-Saavedra E, Lamb J, Peck D, et al. MicroRNA expression profiles classify human cancers. Nature 2005;435:834–8.
21. Ma L, Teruya-Feldstein J, Weinberg RA. Tumour invasion and metastasis initiated by microRNA-10b in breast cancer. Nature 2007;449:682–8.
22. Chang TC, Yu D, Lee YS, Wentzel EA, Arking DE, West KM, et al. Widespread microRNA repression by Myc contributes to tumorigenesis. Nat Genet 2008;40:43–50.
23. Meng F, Henson R, Wehbe-Janek H, Ghoshal K, Jacob ST, Patel T. MicroRNA-21 regulates expression of the PTEN tumor suppressor gene in human hepatocellular cancer. Gastroenterology 2007;133:647–58.
24. Hermeking H. p53 enters the microRNA world. Cancer Cell 2007;12:414–8.
25. Raver-Shapira N, Marciano E, Meiri E, Spector Y, Rosenfeld N, Moskovits N, et al. Transcriptional activation of miR-34a contributes to p53-mediated apoptosis. Mol Cell 2007;26:731–43.
26. He L, He X, Lim LP, de Stanchina E, Xuan Z, Liang Y, et al. A microRNA component of the p53 tumour suppressor network. Nature 2007;447:1130–4.
27. Tazawa H, Tsuchiya N, Izumiya M, Nakagama H. Tumor-suppressive miR-34a induces senescence-like growth arrest through modulation of the E2F pathway in human colon cancer cells. Proc Natl Acad Sci U S A 2007;104:15472–7.
28. Yamakuchi M, Ferlito M, Lowenstein CJ. miR-34a repression of SIRT1 regulates apoptosis. Proc Natl Acad Sci U S A 2008;105:13421–6.
29. Izumiya M, Okamoto K, Tsuchiya N, Nakagama H. Functional screening using a microRNA virus library and microarrays: a new high-throughput assay to identify tumor-suppressive microRNA. Carcinogenesis 2010;31:1354–9.
30. Bunz F, Dutriaux A, Lengauer C, Waldman T, Zhou S, Brown JP, et al. Requirement for p53 and p21 to sustain G2 arrest after DNA damage. Science 1998;282:1497–501.

Published OnlineFirst May 12, 2011; DOI:10.1158/0008-5472.CAN-10-2475

31. Karginov FV, Conaco C, Xuan Z, Schmidt BH, Parker JS, Mandel G, et al. A biochemical approach to identifying microRNA targets. Proc Natl Acad Sci U S A 2007;104:19291–6.
32. Suzuki HI, Yamagata K, Sugimoto K, Iwamoto T, Kato S, Miyazono K. Modulation of microRNA processing by p53. Nature 2009;460:529–33.
33. Sims RJ 3rd, Reinberg D. Histone H3 Lys 4 methylation: caught in a bind? Genes Dev 2006;20:2779–86.
34. Lewis BP, Burge CB, Bartel DP. Conserved seed pairing, often flanked by adenosines, indicates that thousands of human genes are microRNA targets. Cell 2005;120:15–20.
35. Abbas T, Dutta A. p21 in cancer: intricate networks and multiple activities. Nat Rev Cancer 2009;9:400–14.
36. Lazebnik YA, Kaufmann SH, Desnoyers S, Poirier GG, Earnshaw WC. Cleavage of poly(ADP-ribose) polymerase by a proteinase with properties like ICE. Nature 1994;371:346–7.
37. McDonald ER 3rd, Wu GS, Waldman T, El-Deiry WS. Repair defect in p21 WAF1/CIP1 −/− human cancer cells. Cancer Res 1996;56:2250–5.
38. Chang BD, Xuan Y, Broude EV, Zhu H, Schott B, Fang J, et al. Role of p53 and p21waf1/cip1 in senescence-like terminal proliferation arrest induced in human tumor cells by chemotherapeutic drugs. Oncogene 1999;18:4808–18.
39. Choong ML, Yang H, Lee MA, Lane DP. Specific activation of the p53 pathway by low dose actinomycin D: a new route to p53 based cyclotherapy. Cell Cycle 2009;8:2810–8.
40. An WG, Kanekal M, Simon MC, Maltepe E, Blagosklonny MV, Neckers LM. Stabilization of wild-type p53 by hypoxia-inducible factor 1alpha. Nature 1998;392:405–8.
41. Viale A, De Franco F, Orleth A, Cambiaghi V, Giuliani V, Bossi D, et al. Cell-cycle restriction limits DNA damage and maintains self-renewal of leukaemia stem cells. Nature 2009;457:51–6.
42. Enge M, Bao W, Hedstrom E, Jackson SP, Moumen A, Selivanova G. MDM2-dependent downregulation of p21 and hnRNP K provides a switch between apoptosis and growth arrest induced by pharmacologically activated p53. Cancer Cell 2009;15:171–83.
43. Idogawa M, Sasaki Y, Suzuki H, Mita H, Imai K, Shinomura Y, et al. A single recombinant adenovirus expressing p53 and p21-targeting artificial microRNAs efficiently induces apoptosis in human cancer cells. Clin Cancer Res 2009;15:3725–32.
44. Mavrakis KJ, Wolfe AL, Oricchio E, Palomero T, de Keersmaecker K, McJunkin K, et al. Genome-wide RNA-mediated interference screen identifies miR-19 targets in Notch-induced T-cell acute lymphoblastic leukaemia. Nat Cell Biol 2010;12:372–9.
45. Rajewsky N. microRNA target predictions in animals. Nat Genet 2006;38Suppl: S8–S13.
46. Pandey DP, Picard D. miR-22 inhibits estrogen signaling by directly targeting the estrogen receptor alpha mRNA. Mol Cell Biol 2009;29:3783–90.
47. Xiong J, Yu D, Wei N, Fu H, Cai T, Huang Y, et al. An estrogen receptor alpha suppressor, microRNA-22, is downregulated in estrogen receptor alpha-positive human breast cancer cell lines and clinical samples. FEBS J 2010;277:1684–94.
48. Poliseno L, Salmena L, Riccardi L, Fornari A, Song MS, Hobbs RM, et al. Identification of the miR-106b~25 microRNA cluster as a proto-oncogenic PTEN-targeting intron that cooperates with its host gene MCM7 in transformation. Sci Signal 2010; 3:ra29.
49. Cornelis RS, van Vliet M, Vos CB, Cleton-Jansen AM, van de Vijver MJ, Peterse JL, et al. Evidence for a gene on 17p13.3, distal to TP53, as a target for allele loss in breast tumors without p53 mutations. Cancer Res 1994;54:4200–6.
50. Konishi H, Takahashi T, Kozaki K, Yatabe Y, Mitsudomi T, Fujii Y, et al. Detailed deletion mapping suggests the involvement of a tumor suppressor gene at 17p13.3, distal to p53, in the pathogenesis of lung cancers. Oncogene 1998;17:2095–100.

Cancer Science
The official journal of the Japanese Cancer Association JCA

Review Article

Systematic exploration of cancer-associated microRNA through functional screening assays

Masashi Izumiya,[1,3] Naoto Tsuchiya,[1] Koji Okamoto[2] and Hitoshi Nakagama[1,4]

[1]Division of Cancer Development System, [2]Division of Cancer Differentiation, National Cancer Center Research Institute, Tokyo; [3]Department of Gastroenterology, The University of Tokyo Hospital, Tokyo, Japan

(Received January 31, 2011/Revised June 1, 2011/Accepted June 8, 2011/Accepted manuscript online June 11, 2011/Article first published online July 12, 2011)

MicroRNA (miRNA), non-coding RNA of approximately 22 nucleotides, post-transcriptionally represses expression of its target genes. miRNA regulates a variety of biological processes such as cell proliferation, cell death, development, stemness and genomic stability, not only in physiological conditions but also in various pathological conditions such as cancers. More than 1000 mature miRNA have been experimentally identified in humans and mice, yet the functions of a vast majority of miRNA remain to be elucidated. Identification of novel cancer-associated miRNA seems promising considering their possible application in the development of novel cancer therapies and biomarkers. Currently, there are two major approaches to identify miRNA that are associated with cancer: expression profiling study and functional screening assay. The former approach is widely used, and a large number of studies have shown aberrant miRNA expression profiles in cancer tissues compared with their non-cancer counterparts. Although aberrantly expressed miRNA are potentially good biomarkers, in most cases a majority of them do not play causal roles in cancers when functional assays are performed. In contrast, the latter approach allows screening of 'driver' miRNA with cancer-associated phenotypes, such as cell proliferation and cell invasion. Thus, this approach might be suitable in finding crucial targets of novel cancer therapy. The combination of both types of approaches will contribute to further elucidation of the cancer pathophysiology and to the development of a novel class of cancer therapies and biomarkers. (*Cancer Sci* 2011; 102: 1615–1621)

MicroRNA (miRNA) belongs to a class of non-coding RNA of approximately 22 nucleotides, and post-transcriptionally represses expression of its target genes.[1] miRNA are sequentially processed from precursors, either primary transcripts transcribed from the genome or intronic sequences of protein coding genes ('miRtrons'), by RNase III nuclease Drosha and Dicer. After their processing, miRNA are incorporated into the RNA-induced silencing complex (RISC), and the formed complex in turn represses the expression of the target genes, which have partially complimentary sequences with the miRNA in their 3′ untranslated regions (UTR), either by translational repression or cleavage of the target mRNA.[2] Although 3′ UTR is the main target of miRNA, 5′ UTR and open reading frames (ORF) were also reported as target sites of miRNA.[3] More than 60% of all protein coding genes have conserved miRNA binding sites in their 3′ UTR and are implicated to be the targets of miRNA.[4,5]

While miRNA was initially identified in *Caenorhabditis elegans*, it has been demonstrated that miRNA are evolutionarily conserved in many species, suggesting their universal roles in the regulation of gene expression.[6] The number of miRNA whose expression has been experimentally verified has grown rapidly over the last decade. This is partly because the use of sequencing-by-synthesis technology enabled the identification of novel miRNA with low-level expression.[7,8] Currently, 19 724 mature miRNA from 153 species are registered at the miRNA database (miRBase release 17, http://www.mirbase.org), including 1733 (1424 miRNA genes) in the human and 1111 (720 miRNA genes) in the mouse.[9] However, the functions of the vast majority of these miRNA remain to be elucidated. Because the roles of a miRNA depend on its target mRNA and the consequence of repressing multiple target mRNA under a specific cellular condition is difficult to predict, it is necessary to explore miRNA functions under experimental conditions of interest.

miRNA and cancer

It is estimated that more than 60% of all protein coding genes are the potential targets of miRNA.[4,5] Naturally the reported roles of miRNA are implicated in almost all aspects of cellular functions, including cell differentiation, cell death, cell cycle, developmental timing, inflammation, metabolism and stemness.[10–15] As expected from their involvement in normal physiological functions, dysregulation of miRNA expression has been shown to be involved in the pathogenesis of a wide variety of pathological conditions, such as heart disease, neurodegenerative disease and cancer. The dysregulation of miRNA is implicated in almost all aspects of cancer characteristics, including cell cycle, apoptosis, invasion/metastasis, angiogenesis and hypoxia-resistance.

The first evidence that miRNA is involved in the pathogenesis of cancer was obtained from the study of chronic lymphocytic leukemia (CLL), in which *miR-15a* and *miR-16-1* were identified on a region of the genome that was frequently lost in CLL patients.[16] These miRNA target anti-apoptotic protein BCL2, and their downregulation promotes cancers. Hence, it was proposed that these miRNA have a 'tumor-suppressive' role in the pathogenesis of CLL.[17] Since then, a number of reports have demonstrated the involvement of miRNA in cancers (Table 1).

Whereas miR-15a and miR-16-1 were identified through the study of aberrant chromosomes, most cancer-associated miRNA have been identified through expression analyses of miRNA in cancer tissues or by a 'candidate approach' in which potential cancer-associated miRNA that target known oncogenes or tumor-suppressor genes are evaluated as to whether they have cancer-related phenotypes. Interestingly, some miRNA in turn are directly regulated by cancer-associated transcriptional factors, including Myc, HIF, Stat3, p53 and Twist.[18] Thus, the emerging

[4]To whom correspondence should be addressed.
E-mail: hnakagam@ncc.go.jp

doi: 10.1111/j.1349-7006.2011.02007.x

Table 1. Cancer-associated miRNA

Phenotype	miRNA	Function	References
Cell cycle	miR-16	Suppress CDK6, CARD10, CDC27; induce G0/G1 accumulation	41
	miR-17-92	Suppress E2Fs	42
	miR-27a	Suppress Myt-1	43
	miR-34a	Suppress Cdk4/6, cyclin E2, E2F3	20
	miR-122a	Suppress cyclinG1	44
	miR-124a	Suppress CDK6	45
	miR-221/-222	Suppress p27(Kip)	46
	let-7	Suppress Cdk6, Cdc25a, Cyclin D2; induce G0/G1 accumulation	41
Apoptosis	miR-15a/16-1	Suppress Bcl-2; induce apoptosis	17
	miR-22	Suppress p21; induce apoptosis in p53 wild cells	40
	miR-29b	Suppress Mcl-1; suppress apoptosis	47
	miR-34a/b/c	Suppress Bcl-2; induce apoptosis	20
Invasion/ metastasis	miR-10b	Suppress HOXD10; promote invasion/ metastasis	48
	miR-21	Suppress PTEN, Pdcd4; promote motility/ invasion	49
	miR-125a/b	Suppress ERBB2/3; suppress motility/ invasion	50
Angiogenesis	miR-27a	Suppress Zbdb10, promote angiogenesis	43
	miR-17-92	Suppress Tsp1, CTGF; promote angiogenesis	42
	miR-296	Suppress HGS: promote angiogenesis	51
	miR-378	Suppress SuFu, Fus-1; promote angiogenesis	52
Oncogene-associated miRNA	Myc	miR-9, miR-17-92	42
	E2F	miR-17-92	42
	Stat3	miR-21	53
	Twist	miR-10b	48
Tumor-suppressor-associated miRNA	p53	miR-26a, -34, -30c, -103, -107, -182, etc.	18

picture indicates that miRNA and transcriptional factors form an intertwined network during the development of cancers.

Oncogenic miRNA and tumor-suppressive miRNA. miRNA associated with the pathogenesis of cancers can either be classified as oncogenic miRNA (oncomiR) or tumor-suppressive miRNA, although their roles are sometimes dependent on cellular context. As suggested by their name, oncogenic miRNA promote phenotypes associated with cancers, including cell proliferation, invasion and resistance to apoptosis. OncomiR are in many cases upregulated in cancers, and their elevated expression is indispensable for sustained growth of cancer cells.[19] Therefore, inhibition of these miRNA by anti-miRNA can be a new class of molecular-targeted therapy.

In contrast, tumor-suppressive miRNA are miRNA that have anti-tumor functions. Among them is the miR-34 family that represses E2F3, Cdk4, Bcl2 and MET in response to genotoxic stress.[20–22] Of note, miR-34 is a downstream effector of p53, and introduction of miR-34 in cancer cells induces either apoptosis or premature senescence. MiR-34a upregulates p53 by translational repression of SIRT1, thus miR-34a and p53 constitute a positive feedback loop.[23]

Interestingly, miRNA are globally downregulated in many cancer tissues compared with their non-cancerous counterparts.[24] Knockdown of miRNA processing components promote cellular transformation and tumor growth *in vitro* and *in vivo*.[25] Furthermore, reduced expression of Dicer in a subset of lung cancer has been shown to be associated with poor prognosis.[26] These observations suggest that there exists a subset of unidentified miRNA whose downregulation promotes cancer development. Identification of such tumor-suppressive miRNA will be a promising area of future cancer research.

Identification of cancer-associated miRNA for clinical application

Because oncogenic and tumor-suppressive miRNA confer cancer-promoting or cancer-suppressing characteristics to cancers, these miRNA are regarded as potential targets for novel cancer therapies. In addition, aberrantly expressed miRNA can be used for the diagnosis of cancers. Considering that the functions of a substantial proportion of miRNA are not known, systematic exploration of cancer-associated miRNA might be beneficial to detect such clinically relevant miRNA. There are currently two major approaches to explore cancer-associated miRNA: expression analysis and functional assay.

Elucidation of cancer-associated miRNA through expression profiling. A body of evidence indicated there is a number of miRNA aberrantly expressed in cancer tissues in comparison with their non-cancerous counterparts (Table 1). Currently there are several techniques available for miRNA expression analysis including cloning, northern blotting, serial analysis of gene expression (SAGE), microarray, quantitative RT-PCR, *in situ* hybridization and sequencing-by-synthesis technology. Analyses of aberrant chromosomes and methylation status have also been performed to elucidate the underlying mechanisms of aberrant miRNA expression.[16,27] Among them, microarray is an experimental technique that is most widely used for genome-wide miRNA expression profiling. miRNA appear to be relatively stable in various storage conditions of cancer tissues, including fresh frozen tissues and formalin-fixed paraffin-embedded tissues. The relative stability of miRNA makes them good candidates for biomarkers, and expression profiling of miRNA by microarray has become an intense focus of current cancer research.[28] miRNA can also be detected in body fluids, especially blood, and they exhibit altered expression profiles in cancer patients, making them a new class of biomarker.[29–32]

Microarrays have been successfully used for genome-wide expression profiling of miRNA as well as protein-coding genes. However, there have been some technical drawbacks for microarray analysis of miRNA. Because mature miRNA are as short as ~22 nucleotides and members of a miRNA family are highly similar, discrimination of mature miRNA and their precursors is necessary for precise expression profiling of mature miRNA. To overcome the problem, several novel technologies are beginning to emerge for miRNA profiling, including the use of hairpin-structured or locked-nucleic acid (LNA) probes, length-adjusted probes and microfluidics platforms.[33–35] Another drawback of microarray analyses of miRNA is its lack of a proper normalization method. Because of such drawback of the microarray, quantitative RT-PCR (qRT-PCR) is widely used for the quantification of individual miRNA as well as genome-wide miRNA profiling.

doi: 10.1111/j.1349-7006.2011.02007.x

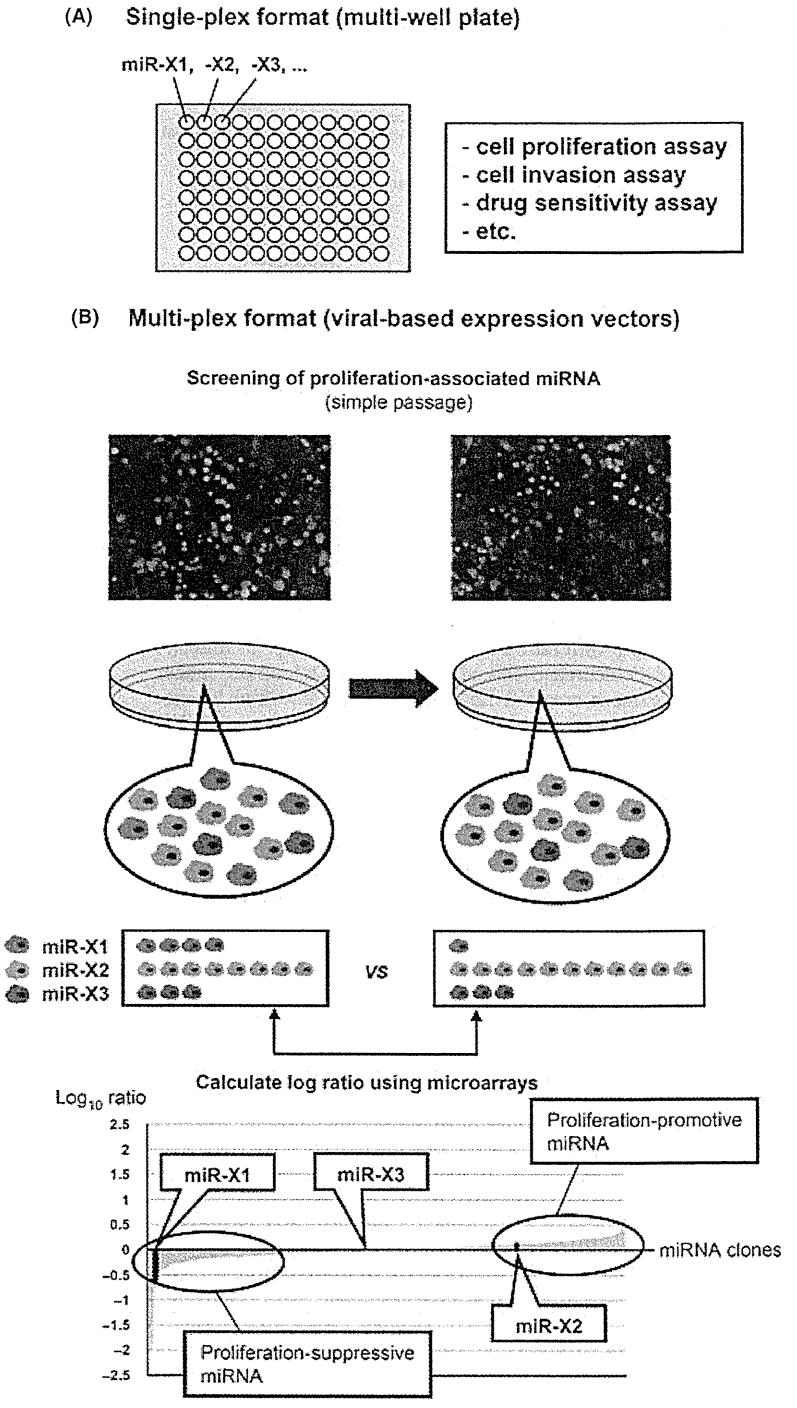

Fig. 1. Schematic view of the functional screening assays. In a single-plex format (A), miRNA undergo functional assays (e.g. cell proliferation assay, cell invasion assay, drug sensitivity assay, etc.) individually in separate wells of a multi-well plate. In a multi-plex format with viral-based expression vectors (B), a large number of cells are infected with a virus library expressing miRNA and then undergo phenotypic screening (e.g. cell proliferation). In the screening of proliferation-associated miRNA, cells transduced with each miRNA clone change their proportions in the whole cell population according to their effects on cell proliferation, which can be quantified using microarrays. For example, cells transduced with a proliferation-suppressive miRNA (miR-X1) or a proliferation-promotive miRNA (miR-X2) increase or decrease their proportion, respectively.

Alternative approach to detect cancer-associated miRNA: functional screening assay of miRNA

Another approach to elucidating miRNA that are associated with cancers is a functional screening assay (Fig. 1).[36–38] This is an assay that enables identification of miRNA that are causally linked to phenotypes of interest, irrespective of their levels of expression. Although there are several methodological variations among these assays, they are basically composed of the following two steps: (i) systematic introduction of miRNA into cells; and (ii) detection of exogenously introduced miRNA that confer cancer-associated phenotypes. Either the arrayed single-plex assay or the pooled multi-plex format with a virus-based expression vector is available for the functional screening assay of miRNA (Table 2).

Single-plex format using multi-well plate. In a single-plex assay, each miRNA is individually introduced to cells and their effects on cells are separately examined in a functional assay in multi-well plates (i.e. 96-well or 384-well format). Synthetic miRNA-mimics or vector-based miRNA can be used under this setting (Table 3). Using 319 synthetic miRNA in a 96-well plate format and chronometric cell viability assay, Nakano *et al.*[37]

Table 2. Representative cancer-associated phenotypes assayed in the functional screening assays of miRNA and genome-wide RNAi screening

	miRNA	RNAi
Array based (single-plex)	Cell proliferation/survival[54]	Partners of *KRAS*[55]
Pool based (multi-plex)	Cell proliferation/survival[36]	Cell proliferation/survival[56–58]
	Cellular transformation[38]	Resistance to nutlin-3[59]
	Cell migration and invasion[60]	p53-dependent proliferation arrest[61]
		Resistance to chemotherapy[62]
		Suppressor of epithelial cell transformation[63,64]
		Tumor suppressor in a mouse lymphoma model[65]

conducted single-plex gain-of-function analysis of miRNA associated with cell proliferation and identified a number of miRNA that increase or decrease cell viability in DLD-1 colon cancer cells. Among them are miR-362, -491 and -132, which do not exhibit aberrant expression in clinical colorectal cancer (CRC) samples.

Multi-plex format with viral-based expression vectors. A pooled multi-plex format with a virus-based expression vector is more complex but can be used for a wide range of applications.[39] Vector-based miRNA, especially those expressing miRNA precursors by retrovirus- or lentivirus-based vectors, are generally used in multi-plex assays, and stable expression of introduced miRNA allows functional screening under various experimental settings (Table 3). In general, a pooled library of miRNA is transduced to a single large cell population and biological selection of the transduced cells is performed. After selecting a cell sub-population with a phenotype of interest, miRNA that cause phenotypic changes are identified by sequencing. Although the viral-based approach has been successfully used to detect oncogenes or OncomiR, in general detection of these factors relies on the growth advantage they confer, and it is difficult to detect anti-miR via such an approach.

An alternative approach to identify cancer-related miRNA from library-transduced cells was initially demonstrated by Voorhoeve *et al.*[38] Genetic screening of miRNA was performed using a retrovirus library of miRNA precursors (~500 bp) and DNA barcode arrays. They successfully identified miR-372 and miR-373 as oncogenic miRNA that cooperate with oncogenic K-ras mutation in immortalized primary fibroblasts (BJ/ET cells). This is an example of the positive screening assay in which a cell population with phenotypes of interest (e.g. cell proliferation) increases during the selection process and the responsible clones are identified either by sequencing or microarrays. The combination of the miRNA-expressing virus library and the custom-made microarray can be used in the negative screening assay ('drop-out' screening) in which a cell population decreases in the selection process.

We have successfully identified miRNA that negatively regulate cell proliferation in pancreatic cancer cells using a lentivirus library of ~450 miRNA precursors and custom-made microarray.[36] Changes in the relative abundance of a miRNA clone (e.g. miR-X1) in the whole cell population were quantified by the comparison of differently labeled miRNA clones recovered

Table 3. Representative commercially available miRNA library

	Species	Structure
Synthetic miRNA-like molecules		
miRNA mimic (gain-of-function analysis)		
Pre-miR miRNA precursor molecule (Ambion, Austin, TX, USA)	H, M	Double stranded
miRIDIAN microRNA Mimic (Thermo Fisher Scientific, Lafayette, CO, USA)	H, M, R	Double stranded
miScript miRNA Mimics (Qiagen, Hilden, Germany)	H, M, R	Double stranded
MISSION (Sigma-Aldrich, St. Louis, MO, USA)	H	Double stranded
miRNA inhibitor (loss-of-function analysis)		
miRCURY LNA microRNA inhibitor (Exiqon, Vedbaek, Denmark)	H, M	Single stranded
Anti-miR miRNA inhibitors (Ambion)	H, M	Single stranded
miRIDIAN microRNA hairpin inhibitor (Thermo Fisher Scientific)	H, M, R	Single stranded
miScript miRNA inhibitors (Qiagen)	H, M, R	Single stranded
miArrest (GeneCopoeia, Rockville, MD, USA)	H, M, R	Single stranded
Virus vector-based miRNA		
miRNA (gain-of-function analysis)		
Virus vector		
(non-barcoded)		
Lenti-miR microRNA (System Biosciences, Mountain View, CA, USA)	H	HIV based, expressing miRNA precursors
miRNA library (miR-Lib) (NKI, Amsterdam, The Netherlands)	H	MSCV based, expressing miRNA precursors
miExpress (GeneCopoeia)	H, M, R	FIV based, expressing miRNA stem-loop
miRIDIAN shMIMIC microRNA (Thermo Fisher Scientific)	H	HIV based, expressing mature miRNA incorporated into a universal scaffold
Non-viral vector		
miExpress (GeneCopoeia)	H, M, R	Non-viral vector expressing miRNA precursor
miRNA inhibitor (loss-of-function analysis)		
miRZIP (System Biosciences)	H	HIV based
miArrest (GeneCopoeia)	H, M, R	HIV based

FIV, feline immunodeficiency virus; H, human; HIV, human immunodeficiency virus; M, mouse; MSCV, murine stem cell virus; R, rat.

doi: 10.1111/j.1349-7006.2011.02007.x

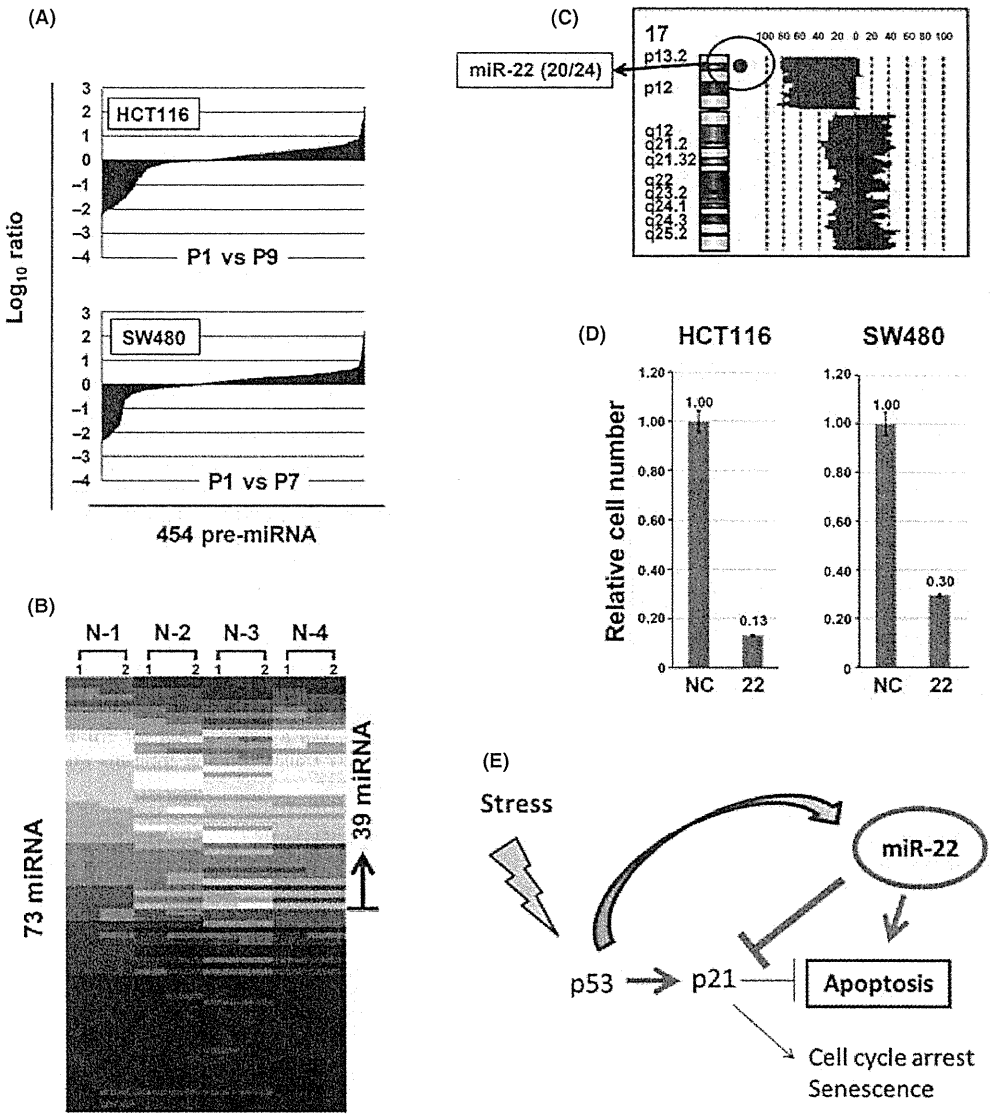

Fig. 2. (A) Results of dropout screening. HCT116 and SW480 cells were transduced with a lentivirus pooled miRNA expression library at multiplicity of infection (MOI) of 3. Exogenous transduced miRNA precursor genes were PCR amplified from genomic DNA recovered from cells immediately after library infection (passage 1, P1) and after several passages (P9 in HCT 116 cells and P7 in SW480 cells). Amplified DNA were labeled with Cy3 (P1) and Cy5 (P9 and P7), and competitively hybridized onto a custom-made microarray. Graphs are a scattered plot of the $\log_{10}$ ratio of each array set. (B) Expression profile of miRNA in non-cancerous parts of four colon cancer specimens using microarrays. A heat map was made using expression levels of 73 dropout miRNA. (C) Copy number aberration of chromosome 17 in 24 human colon cancer patients. Green and red indicate loss and gain, respectively. The position of the miR-22 gene is shown by the red dot. (D) Cell proliferation assay. HCT 116 and SW480 cells were transfected with 5 nM of either miR-negative control (NC) or miR-22 (22) and incubated for 5 days. Cell viability was measured by MST (Promega, Fitchburg, WI, USA) assay. Error bars indicate standard deviation in triplicate cultures. (E) Possible roles of miR-22 as an intrinsic molecular switch. In the exposure to oncogenic stresses, activated p53 transcriptionally activates both p21 and miR-22. MiR-22 represses p21 directly through the inhibition of translation and enhancement of mRNA degradation. Repression of p21 might cause the changes of cellular state from cell cycle arrest to apoptosis.

immediately after infection or after several passages (Fig. 1B). Five miRNA exhibited remarkable reduction in their abundance ($\log_{10}$ ratio <-1), indicating the proliferation-suppressive effect of these miRNA. Interestingly, one of these five miRNA was miR-34a, a representative tumor-suppressive miRNA that is transactivated by p53.[20,21] MiR-34a does not exhibit aberrant expression in pancreatic cancers or it exhibits mild upregulation in colorectal cancers. We have also reported that miR-222, which is upregulated in pancreatic cancers and has been shown to be tumor promotive by targeting p27, PUMA and PPP2R2A, has a tumor-suppressive effect in pancreatic cancer cells. These results suggest a methodological advantage of this functional screening assay to detect hidden cancer-related genes, and illustrates the need to explore miRNA functions in various tissues as the functions of miRNA are sometimes context-dependent, further showing the importance of experimental validation of cancer-associated miRNA using a functional screening assay. The flexibility of a multi-plex format assay also warrants exploration in more complicated settings, including *in vivo* settings. Moreover, use of lentivirus vectors broadens the possible application of the assay to primary or non-dividing cells, including neural and stem cells.

miR-22, a novel tumor-suppressor gene, identified by functional genetic and comprehensive genomic analyses. The usefulness of a functional screening assay in the exploration of tumor suppressive miRNA can further be strengthened by combining the results of the assay with other data, especially those of clinical samples. We integrated the functional screening assay, expression profiling and chromosome analysis to identify miRNA species that function as tumor-suppressor genes in colon cancer[40]. Tumor-suppressor miRNA were defined as miRNA that: (i) repress cell proliferation; (ii) is expressed in normal colon tissues; (iii) is located at a frequently lost region on the chromosome; and (iv) is downregulated in colon cancers. As indicated in Figure 2A, considerable numbers of miRNA clones dropped out during the culture of HCT 116 or SW480 cell lines. Expression analysis of proliferation-suppressive ('drop-out') clones in non-cancerous colon tissues (Fig. 2B) and copy number analysis of colon cancer tissues (Fig. 2C) led to a novel tumor-suppressor miRNA miR-22 that satisfies the aforementioned four criteria.

The activity of repression for cell proliferation was again assessed by the introduction of miR-22 in both HCT 116 and SW480 cells (Fig. 2D). Interestingly, miR-22 induced apoptosis only in p53 wild-type cells, but it caused cell cycle arrest in p53 mutant cells.[40] Furthermore, we found that miR-22 is a transcriptional target of p53 and directly represses p21. Our findings define an intrinsic molecular switch that controls apoptosis by direct repression of p21 in response to strong stresses, in which cells should eliminate severely damaged cells to prevent malignant transformation (Fig. 2E).

In summary, functional screening of miRNA using either a single-plex or multi-plex format is a powerful genetic approach for the systematic elucidation of miRNA that cause cancer-associated phenotypes independent of their expression. Moreover, by combining the functional screening assay with expression profiling and genomic analysis, it should further facilitate the identification of novel cancer-associated miRNA that have a vital role in cancer pathophysiology, such as the miR-34 family and miR-22.

Perspectives

There is growing interest in the clinical application of miRNA. Aberrantly expressed miRNA in cancer tissues are good candidate biomarkers for the diagnosis of cancers and the prognosis of cancer patients, as has been shown by a large number of studies.[18] In addition, they are suitable as a good biomarker because of their ease of detection, high stability in clinical specimens and availability from the blood of cancer patients. Furthermore, miRNA themselves can be a novel class of molecular targets in cancer therapy. In theory, suppression of upregulated oncogenic miRNA by anti-miRNA or introduction of downregulated tumor-suppressive miRNA by synthetic or viral-vector based miRNA might be effective to cure cancer, although the development of effective drug delivery systems is another challenge. Identification of regulators of the mechanisms of cancer-associated miRNA will provide novel therapeutic targets. Despite many obstacles, exploration of cancer-associated miRNA will contribute to the elucidation of the pathogenesis of cancers and the development of novel cancer therapies and biomarkers.

Acknowledgments

This work is supported by the Program for Promotion of Fundamental Studies in Health Sciences of the National Institute of Biomedical Innovation (NIBIO), and a Grant-in-Aid for 3rd Term Comprehensive 10-Year Strategy for Cancer Control from the Ministry of Health, Labour and Welfare, Japan.

Disclosure Statement

The authors have no conflict of interest.

References

1 Bartel DP. MicroRNAs: genomics, biogenesis, mechanism, and function. *Cell* 2004; **116**: 281–97.
2 Filipowicz W, Bhattacharyya SN, Sonenberg N. Mechanisms of post-transcriptional regulation by microRNAs: are the answers in sight? *Nat Rev Genet* 2008; **9**: 102–14.
3 Orom UA, Nielsen FC, Lund AH. MicroRNA-10a binds the 5'UTR of ribosomal protein mRNAs and enhances their translation. *Mol Cell* 2008; **30**: 460–71.
4 Friedman RC, Farh KK, Burge CB, Bartel DP. Most mammalian mRNAs are conserved targets of microRNAs. *Genome Res* 2009; **19**: 92–105.
5 Lewis BP, Burge CB, Bartel DP. Conserved seed pairing, often flanked by adenosines, indicates that thousands of human genes are microRNA targets. *Cell* 2005; **120**: 15–20.
6 Lee RC, Feinbaum RL, Ambros V. The *C. elegans* heterochronic gene lin-4 encodes small RNAs with antisense complementarity to lin-14. *Cell* 1993; **75**: 843–54.
7 Friedlander MR, Chen W, Adamidi C *et al.* Discovering microRNAs from deep sequencing data using miRDeep. *Nat Biotechnol* 2008; **26**: 407–15.
8 Morin RD, O'Connor MD, Griffith M *et al.* Application of massively parallel sequencing to microRNA profiling and discovery in human embryonic stem cells. *Genome Res* 2008; **18**: 610–21.
9 Griffiths-Jones S, Saini HK, van Dongen S, Enright AJ. miRBase: tools for microRNA genomics. *Nucleic Acids Res* 2008; **36**: D154–8.
10 Calin GA, Croce CM. MicroRNA signatures in human cancers. *Nat Rev Cancer* 2006; **6**: 857–66.
11 Melton C, Judson RL, Blelloch R. Opposing microRNA families regulate self-renewal in mouse embryonic stem cells. *Nature* 2010; **463**: 621–6.
12 Valeri N, Gasparini P, Fabbri M *et al.* Modulation of mismatch repair and genomic stability by miR-155. *Proc Natl Acad Sci USA* 2010; **107**: 6982–7.
13 O'Connell RM, Rao DS, Chaudhuri AA, Baltimore D. Physiological and pathological roles for microRNAs in the immune system. *Nat Rev Immunol* 2010; **10**: 111–22.
14 Chen D, Farwell MA, Zhang B. MicroRNA as a new player in the cell cycle. *J Cell Physiol* 2010; **225**: 296–301.
15 Najafi-Shoushtari SH, Kristo F, Li Y *et al.* MicroRNA-33 and the SREBP host genes cooperate to control cholesterol homeostasis. *Science* 2010; **328**: 1566–9.
16 Calin GA, Dumitru CD, Shimizu M *et al.* Frequent deletions and down-regulation of micro-RNA genes miR15 and miR16 at 13q14 in chronic lymphocytic leukemia. *Proc Natl Acad Sci USA* 2002; **99**: 15524–9.
17 Cimmino A, Calin GA, Fabbri M *et al.* miR-15 and miR-16 induce apoptosis by targeting BCL2. *Proc Natl Acad Sci USA* 2005; **102**: 13944–9.
18 Lee YS, Dutta A. MicroRNAs in cancer. *Annu Rev Pathol* 2009; **4**: 199–227.
19 Voorhoeve PM. MicroRNAs: oncogenes, tumor suppressors or master regulators of cancer heterogeneity? *Biochim Biophys Acta* 2010; **1805**: 72–86.
20 He L, He X, Lowe SW, Hannon GJ. microRNAs join the p53 network – another piece in the tumour-suppression puzzle. *Nat Rev Cancer* 2007; **7**: 819–22.
21 Tazawa H, Tsuchiya N, Izumiya M, Nakagama H. Tumor-suppressive miR-34a induces senescence-like growth arrest through modulation of the E2F pathway in human colon cancer cells. *Proc Natl Acad Sci USA* 2007; **104**: 15472–7.
22 Tsuchiya N, Nakagama H. MicroRNA, SND1, and alterations in translational regulation in colon carcinogenesis. *Mutat Res* 2010; **693**: 94–100.
23 Yamakuchi M, Ferlito M, Lowenstein CJ. miR-34a repression of SIRT1 regulates apoptosis. *Proc Natl Acad Sci USA* 2008; **105**: 13421–6.
24 Lu J, Getz G, Miska EA *et al.* MicroRNA expression profiles classify human cancers. *Nature* 2005; **435**: 834–8.
25 Kumar MS, Lu J, Mercer KL, Golub TR, Jacks T. Impaired microRNA processing enhances cellular transformation and tumorigenesis. *Nat Genet* 2007; **39**: 673–7.
26 Karube Y, Tanaka H, Osada H *et al.* Reduced expression of Dicer associated with poor prognosis in lung cancer patients. *Cancer Sci* 2005; **96**: 111–5.
27 Kozaki K, Imoto I, Mogi S, Omura K, Inazawa J. Exploration of tumor-suppressive microRNAs silenced by DNA hypermethylation in oral cancer. *Cancer Res* 2008; **68**: 2094–105.
28 Osaki M, Takeshita F, Ochiya T. MicroRNAs as biomarkers and therapeutic drugs in human cancer. *Biomarkers* 2008; **13**: 658–70.

doi: 10.1111/j.1349-7006.2011.02007.x

29 Ahmed FE, Jeffries CD, Vos PW *et al.* Diagnostic microRNA markers for screening sporadic human colon cancer and active ulcerative colitis in stool and tissue. *Cancer Genomics Proteomics* 2009; **6**: 281–95.
30 Kosaka N, Iguchi H, Ochiya T. Circulating microRNA in body fluid: a new potential biomarker for cancer diagnosis and prognosis. *Cancer Sci* 2010; **101**: 2087–92.
31 Link A, Balaguer F, Shen Y *et al.* Fecal MicroRNAs as novel biomarkers for colon cancer screening. *Cancer Epidemiol Biomarkers Prev* 2010; **19**: 1766–74.
32 Tsujiura M, Ichikawa D, Komatsu S *et al.* Circulating microRNAs in plasma of patients with gastric cancers. *Br J Cancer* 2010; **102**: 1174–9.
33 Wang H, Ach RA, Curry B. Direct and sensitive miRNA profiling from low-input total RNA. *RNA* 2007; **13**: 151–9.
34 Petersen M, Wengel J. LNA: a versatile tool for therapeutics and genomics. *Trends Biotechnol* 2003; **21**: 74–81.
35 Baskerville S, Bartel DP. Microarray profiling of microRNAs reveals frequent coexpression with neighboring miRNAs and host genes. *RNA* 2005; **11**: 241–7.
36 Izumiya M, Okamoto K, Tsuchiya N, Nakagama H. Functional screening using a microRNA virus library and microarrays: a new high-throughput assay to identify tumor-suppressive microRNAs. *Carcinogenesis* 2010; **31**: 1354–9.
37 Nakano H, Miyazawa T, Kinoshita K, Yamada Y, Yoshida T. Functional screening identifies a microRNA, miR-491 that induces apoptosis by targeting Bcl-X(L) in colorectal cancer cells. *Int J Cancer* 2010; **127**: 1072–80.
38 Voorhoeve PM, le Sage C, Schrier M *et al.* A genetic screen implicates miRNA-372 and miRNA-373 as oncogenes in testicular germ cell tumors. *Cell* 2006; **124**: 1169–81.
39 Echeverri CJ, Perrimon N. High-throughput RNAi screening in cultured cells: a user's guide. *Nat Rev Genet* 2006; **7**: 373–84.
40 Tsuchiya N, Izumiya M, Ogata-Kawata H *et al.* Tumor-suppressor miR-22 determines p53-dependent cellular fate through post-transcriptional regulation of p21. *Cancer Res* 2011; doi: 10.1158/0008-5472.CAN-10-2475 [Epub ahead of print].
41 Chivukula RR, Mendell JT. Circular reasoning: microRNAs and cell-cycle control. *Trends Biochem Sci* 2008; **33**: 474–81.
42 Mendell JT. miRiad roles for the miR-17-92 cluster in development and disease. *Cell* 2008; **133**: 217–22.
43 Mertens-Talcott SU, Chintharlapalli S, Li X, Safe S. The oncogenic microRNA-27a targets genes that regulate specificity protein transcription factors and the G2-M checkpoint in MDA-MB-231 breast cancer cells. *Cancer Res* 2007; **67**: 11001–11.
44 Gramantieri L, Ferracin M, Fornari F *et al.* Cyclin G1 is a target of miR-122a, a microRNA frequently down-regulated in human hepatocellular carcinoma. *Cancer Res* 2007; **67**: 6092–9.
45 Agirre X, Vilas-Zornoza A, Jimenez-Velasco A *et al.* Epigenetic silencing of the tumor suppressor microRNA Hsa-miR-124a regulates CDK6 expression and confers a poor prognosis in acute lymphoblastic leukemia. *Cancer Res* 2009; **69**: 4443–53.
46 le Sage C, Nagel R, Egan DA *et al.* Regulation of the p27(Kip1) tumor suppressor by miR-221 and miR-222 promotes cancer cell proliferation. *EMBO J* 2007; **26**: 3699–708.
47 Mott JL, Kobayashi S, Bronk SF, Gores GJ. mir-29 regulates Mcl-1 protein expression and apoptosis. *Oncogene* 2007; **26**: 6133–40.
48 Ma L, Teruya-Feldstein J, Weinberg RA. Tumour invasion and metastasis initiated by microRNA-10b in breast cancer. *Nature* 2007; **449**: 682–8.
49 Asangani IA, Rasheed SA, Nikolova DA *et al.* MicroRNA-21 (miR-21) post-transcriptionally downregulates tumor suppressor Pdcd4 and stimulates invasion, intravasation and metastasis in colorectal cancer. *Oncogene* 2008; **27**: 2128–36.
50 Scott GK, Goga A, Bhaumik D, Berger CE, Sullivan CS, Benz CC. Coordinate suppression of ERBB2 and ERBB3 by enforced expression of micro-RNA miR-125a or miR-125b. *J Biol Chem* 2007; **282**: 1479–86.
51 Wurdinger T, Tannous BA, Saydam O., et al. miR-296 regulates growth factor receptor overexpression in angiogenic endothelial cells. *Cancer Cell.* 2008; **14**: 382–93.
52 Lee DY, Deng Z, Wang CH, Yang BB. MicroRNA-378 promotes cell survival, tumor growth, and angiogenesis by targeting SuFu and Fus-1 expression. *Proc Natl Acad Sci USA* 2007; **104**: 20350–5.
53 Ohno M, Natsume A, Kondo Y *et al.* The modulation of microRNAs by type I IFN through the activation of signal transducers and activators of transcription 3 in human glioma. *Mol Cancer Res* 2009; **7**: 2022–30.
54 Nakano H, Miyazawa T, Kinoshita K, Yamada Y, Yoshida T. Functional screening identifies a microRNA, miR-491 that induces apoptosis by targeting Bcl-X(L) in colorectal cancer cells. *Int J Cancer* 2010; **127**: 1072–80.
55 Barbie DA, Tamayo P, Boehm JS *et al.* Systematic RNA interference reveals that oncogenic KRAS-driven cancers require TBK1. *Nature* 2009; **462**: 108–12.
56 Schlabach MR, Luo J, Solimini NL *et al.* Cancer proliferation gene discovery through functional genomics. *Science* 2008; **319**: 620–4.
57 Silva JM, Marran K, Parker JS *et al.* Profiling essential genes in human mammary cells by multiplex RNAi screening. *Science* 2008; **319**: 617–20.
58 Ngo VN, Davis RE, Lamy L *et al.* A loss-of-function RNA interference screen for molecular targets in cancer. *Nature* 2006; **441**: 106–10.
59 Brummelkamp TR, Fabius AW, Mullenders J *et al.* An shRNA barcode screen provides insight into cancer cell vulnerability to MDM2 inhibitors. *Nat Chem Biol* 2006; **2**: 202–6.
60 Huang Q, Gumireddy K, Schrier M *et al.* The microRNAs miR-373 and miR-520c promote tumour invasion and metastasis. *Nat Cell Biol* 2008; **10**: 202–10.
61 Berns K, Hijmans EM, Mullenders J *et al.* A large-scale RNAi screen in human cells identifies new components of the p53 pathway. *Nature* 2004; **428**: 431–7.
62 Berns K, Horlings HM, Hennessy BT *et al.* A functional genetic approach identifies the PI3K pathway as a major determinant of trastuzumab resistance in breast cancer. *Cancer Cell* 2007; **12**: 395–402.
63 Kolfschoten IG, van Leeuwen B, Berns K *et al.* A genetic screen identifies PITX1 as a suppressor of RAS activity and tumorigenicity. *Cell* 2005; **121**: 849–58.
64 Westbrook TF, Martin ES, Schlabach MR *et al.* A genetic screen for candidate tumor suppressors identifies REST. *Cell* 2005; **121**: 837–48.
65 Bric A, Miething C, Bialucha CU *et al.* Functional identification of tumor-suppressor genes through an *in vivo* RNA interference screen in a mouse lymphoma model. *Cancer Cell* 2009; **16**: 324–35.

$SCF^{\beta TrCP}$ mediates stress-activated MAPK-induced Cdc25B degradation

Sanae Uchida[1], Nobumoto Watanabe[2], Yasusei Kudo[3], Katsuji Yoshioka[4], Tsukasa Matsunaga[5], Yukihito Ishizaka[6], Hitoshi Nakagama[7], Randy Y. C. Poon[8] and Katsumi Yamashita[5,*]

[1]Venture Business Laboratory, Center for Innovation, Kanazawa University, Kakuma, Kanazawa 920-1192, Ishikawa, Japan
[2]Chemical Library Validation Team, Chemical Biology Core Facility, Chemical Biology Department, RIKEN ASI, Wako 351-0198, Saitama, Japan
[3]Department of Oral Maxillofacial Pathobiology, Division of Frontier Medical Science, Graduate School of Medical Sciences, Hiroshima University, Hiroshima 734-8553, Japan
[4]Division of Molecular Cell Signaling, Cancer Research Institute, Kanazawa University, Kakuma, Kanazawa 920-1192, Ishikawa, Japan
[5]Division of Pharmaceutical Sciences, Institute of Medical, Pharmaceutical and Health Sciences, Kanazawa University, Kakuma, Kanazawa 920-1192, Ishikawa, Japan
[6]Division of Intractable Diseases, Research Institute, National Center for Global Health and Medicine, Tokyo 162-8655, Japan
[7]Early Oncogenesis Research Project, National Cancer Center Research Institute, Tokyo 104-0045, Japan
[8]Division of Life Science, The Hong Kong University of Science and Technology, Clear Water Bay, Hong Kong
*Author for correspondence (katsumi@kenroku.kanazawa-u.ac.jp)

Accepted 26 April 2011
Journal of Cell Science 124, 2816-2825

doi:10.1242/jcs.083931

Summary

Cdc25A, which is one of the three mammalian CDK-activating Cdc25 protein phosphatases (Cdc25A, B and C), is degraded through $SCF^{\beta TrCP}$-mediated ubiquitylation following genomic insult; however, the regulation of the stability of the other two Cdc25 proteins is not well understood. Previously, we showed that Cdc25B is primarily degraded by cellular stresses that activate stress-activated MAPKs, such as Jun NH_2-terminal kinase (JNK) and p38. Here, we report that Cdc25B was ubiquitylated by $SCF^{\beta TrCP}$ E3 ligase upon phosphorylation at two Ser residues in the βTrCP-binding-motif-like sequence $D^{94}AGLCMDSPSP^{104}$. Point mutation of these Ser residues to alanine (Ala) abolished the JNK-induced ubiquitylation by $SCF^{\beta TrCP}$, and point mutation of DAG to AAG or DAA eradicated both βTrCP binding and ubiquitylation. Further analysis of the mode of βTrCP binding to this region revealed that the PEST-like sequence from $E^{82}SS$ to $D^{94}AG$ is crucially involved in both the βTrCP binding and ubiquitylation of Cdc25B. Furthermore, the phospho-mimetic replacement of all 10 Ser residues in the $E^{82}SS$ to $SPSP^{104}$ region with Asp resulted in βTrCP binding. Collectively, these results indicate that stress-induced Cdc25B ubiquitylation by $SCF^{\beta TrCP}$ requires the phosphorylation of $S^{101}PS^{103}P$ in the βTrCP-binding-motif-like and adjacent PEST-like sequences.

Key words: Cdc25B, $SCF^{\beta TrCP}$, Phosphorylation, PEST-like

Introduction

Cdc25 dual-specificity phosphatases promote cell cycle progression via the activation of cyclin-dependent kinase (CDK)–cyclin by removing inhibitory phosphate groups on CDK (Morgan, 1995; Boutros et al., 2006). Higher Metazoa possess three isoforms of Cdc25: Cdc25A, B and C. These are largely considered to serve roles in different phases of the cell cycle: Cdc25A in the G1 to S phase, and Cdc25B and C in the G2 to M phase (Boutros et al., 2006). However, this is not strictly correct because the depletion of either one or two *Cdc25* genes does not produce a defective phenotype in the normal cell cycle, indicating that their roles overlap in somatic cell-cycle control (Chen et al., 2001; Lincoln et al., 2002; Ferguson et al., 2005; Ray et al., 2007; Lee et al., 2009).

Of the three mammalian Cdc25 isoforms, Cdc25A has received special attention because it is a target of the DNA replication or damage checkpoint (Donzelli and Draetta, 2003; Bartek et al., 2004) and is the only Cdc25 that is essential to mouse embryogenesis (Ray et al., 2007; Lee et al., 2009). Cdc25A is phosphorylated rapidly by CHK1 upon genomic damage or replication arrest, and this is followed by the phosphorylation of crucial Ser residues in the βTrCP-binding DSG (Asp-Ser-Gly) motif by NEK11 (Busino et al., 2003; Jin et al., 2003; Melixetian et al., 2009), which initiates $SCF^{\beta TrCP}$-mediated ubiquitylation and degradation (Busino et al., 2004). Moreover, Cdc25A is directly linked to tumorigenesis, and the frequent overexpression of Cdc25A in human cancers is well documented (Kristjansdottir and Rudolph, 2004; Boutros et al., 2007).

The WD repeat-containing F-box protein βTrCP is a substrate-binding component of SCF (Skp1–cullin-1–F-box protein) E3 ubiquitin ligase that recognises the doubly phosphorylated conserved motif DSGxxS (S can be replaced by T, and x represents any amino acid) (Winston et al., 1999; Latres et al., 1999). $SCF^{\beta TrCP}$ targets a number of proteins that regulate the cell cycle and apoptosis (Frescas and Pagano, 2008). In particular, some proteins that control the G2–M transition, such as Cdc25A, Emi1, Wee1A and Bora, are $SCF^{\beta TrCP}$ substrates, and most of them contain the above-mentioned βTrCP-binding sequence (Busino et al., 2003; Jin et al., 2003; Margottin-Goguet et al., 2003; Guardavaccaro et al., 2003; Watanabe et al., 2004; Seki et al., 2008). Wee1 kinase is also a substrate of $SCF^{\beta TrCP}$, but its proposed βTrCP-binding sequence deviates from the consensus sequence (Watanabe et al., 2004). The consensus sequence and its deviated phosphopeptides bind βTrCP by forming hydrogen bonds and electrostatic interactions (Wu et al., 2003). In addition to such phosphopeptides, Cdc25A and Cdc25B possess the non-phosphorylated βTrCP-binding sequence DDGxxD (Kanemori et al., 2005).

Similar to Cdc25A, Cdc25B can transform retinoblastoma-protein-negative cells or normal cells when coexpressed with the oncogenic Ras (Galaktionov et al., 1995). Cdc25B overexpression is also found in human cancers and is correlated with a poor prognosis, as in the case of Cdc25A (Kristjansdottir and Rudolph, 2004; Boutros et al., 2007). The tumorigenic activity of Cdc25B is partly explained by an increase in hyperplasia or susceptibility to carcinogens in Cdc25B transgenic mice (Ma et al., 1999; Yao et al., 1999). Moreover, Cdc25B overexpression accelerates mitotic entry (Karlsson et al., 1999) and overrides the radiation-induced G2 checkpoint in vitro (Miyata et al., 2001).

Recently, we showed that Cdc25B is degraded rapidly by non-genotoxic stimuli that activate stress-responsive MAPKs, such as Jun N-terminal kinase (JNK) and p38 (Uchida et al., 2009). Our results suggested that these kinases phosphorylate specific Ser residues in the N-terminal region (S101 and S103) to induce Cdc25B degradation. We also found that HeLa cells expressing the non-phosphorylatable S101A mutant Cdc25B were more refractory to anisomycin-induced G2 arrest than wild-type HeLa cells.

Here, we report that JNK-induced Cdc25B ubiquitylation is mediated by the F-box protein βTrCP-containing SCF ubiquitin ligase. We show that S101 and S103 are phosphorylated upon non-genotoxic stress and that βTrCP binds the sequence around S101 and S103 of Cdc25B in a phosphorylation-dependent manner, even when the DSG consensus βTrCP-binding sequence is replaced with DAG. Our data also indicate that full binding and ubiquitylation of Cdc25B by SCF$^{\beta TrCP}$ requires an upstream ESS (Glu-Ser-Ser)-rich PEST-like sequence, as well as DAG and S101 and S103 phosphorylation.

Results

Ubiquitylation of Cdc25B is carried out by SCF$^{\beta TrCP}$ and is controlled by JNK

Our previous report suggested that non-genotoxic stress-induced Cdc25B degradation was mediated by the ubiquitin–proteasome pathway via S101 and S103 phosphorylation by JNK or p38 (Uchida et al., 2009). Fig. 1A shows that the amino acid sequence surrounding S101 and S103 of Cdc25B is similar to that in Cdc25A, which is a substrate of SCF$^{\beta TrCP}$ E3 ubiquitin ligase (Busino et al., 2003; Jin et al., 2003). Despite the overall similarity, the crucial βTrCP-binding motif of Cdc25A (DSG) is replaced with DAG in Cdc25B, and DAG is reported to be inactive for βTrCP binding in humans and *Xenopus* Cdc25A (Busino et al., 2003; Jin et al., 2003; Kanemori et al., 2005).

The corresponding region of Cdc25B, including the human splice variants Cdc25B2 and Cdc25B3 and mouse Cdc25B1, has a similar amino acid sequence (Fig. 1A) (Baldin et al., 1997; Kakizuka et al., 1992). As indicated in Fig. 1B, human Cdc25B3,

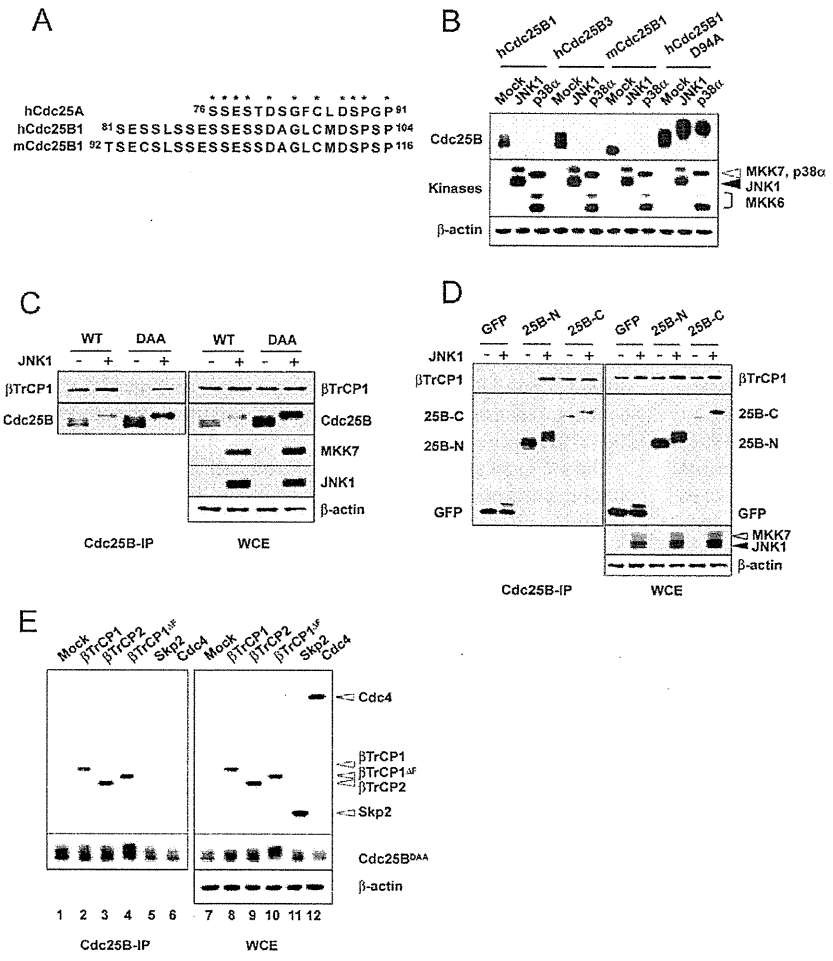

Fig. 1. βTrCP binds Cdc25B. (**A**) The aligned amino acid sequences of human (h) and mouse (m) Cdc25B and human Cdc25A, required for βTrCP binding. Asterisks indicate amino acids common to all three peptides. (**B**) Each FLAG-tagged cDNA of human Cdc25B1 and B3 and mouse Cdc25B1 was co-transfected with either JNK1 and its activator MKK7 or p38α and its activator MKK6, followed by immunoblotting to detect the expression of the indicated proteins (JNK1 or p38α was co-transfected with its respective activator, MKK7 or MKK6, unless stated otherwise and the coexpression of JNK1 and MKK7 or p38α with MKK6 is shown as JNK1 or p38, respectively, thereafter). The expression of human Cdc25B1 with a mutation at D94 to A of DAG (D94A) was also determined. (**C**) Either a FLAG–Cdc25B^{WT} or FLAG–Cdc25B^{DAA} with mutations in the constitutive βTrCP-binding sequence DDG was co-transfected with Myc-βTrCP1 in the presence or absence of JNK1. Then, 24 hours later, either Cdc25B binding to βTrCP1 or recovered Cdc25B was determined by immunoprecipitation with anti-FLAG beads, followed by immunoblotting with anti-Myc or anti-FLAG antibodies (Cdc25B-IP lanes). The expression of the indicated proteins is also shown (WCE lanes). (**D**) The βTrCP1 binding to Cdc25B fragments of the N-terminal 175 amino acids (1–175; 25B–N) or C-terminal fragment (180–580; 25B–C), both of which contain an N-terminal FLAG tag and C-terminal GFP tag, was examined as described in C. FLAG–GFP was used as a control (Cdc25B-IP lanes). The expression of the indicated proteins is shown (WCE lanes). (**E**) FLAG–Cdc25B^{DAA} and Myc-tagged F-box proteins were co-transfected and their interaction was determined by immunoprecipitation and immunoblotting. The interaction between Cdc25B^{DDA} and βTrCP1$^{\Delta F}$ lacking an F-box sequence was also determined (Cdc25B-IP lanes). The expression of the indicated proteins is also shown (WCE lanes).

mouse Cdc25B1 and human Cdc25B1 were also degraded on coexpression with JNK or p38 (hereafter, we refer to human Cdc25B1 as Cdc25B). Interestingly, the Cdc25B D94A mutant was refractory to JNK- or p38-induced degradation, suggesting the involvement of βTrCP binding (Fig. 1B).

Next, we investigated the JNK-dependent interaction between βTrCP1 and Cdc25B. We compared βTrCP binding to the Cdc25B of the wild type and a mutant that lacked the constitutive βTrCP-binding motif by mutating $D^{254}DG$ to DAA, which hereafter is referred to as $Cdc25B^{DAA}$. Although wild-type Cdc25B bound βTrCP1 irrespective of the JNK activity, $Cdc25B^{DAA}$ interacted with βTrCP1 in a JNK-dependent manner (Fig. 1C). JNK induced wild-type Cdc25B degradation and apparent Cdc25B binding was not enhanced. Given the JNK-induced wild-type Cdc25B degradation that occurred, several times more βTrCP was estimated to bind Cdc25B on coexpression with JNK. Likewise, the Cdc25B N-terminal fragment displayed JNK-dependent βTrCP1 binding, whereas the C-terminal fragment with the DDG site showed that βTrCP bound in a JNK-independent manner (Fig. 1D). Furthermore, $Cdc25B^{DAA}$ interacted with βTrCP1 and βTrCP2, but not with other F-box proteins such as Skp2 and Cdc4 (Fig. 1E). $Cdc25B^{DAA}$ was stabilised when co-transfected with the F-box deletion mutant $βTrCP1^{ΔF}$, which lacks ubiquitylation activity because of its inability to bind to the core SCF complex, but retains substrate-binding ability via an intact WD domain (Fig. 1E).

Next, we investigated the ubiquitylation of Cdc25B by $SCF^{βTrCP}$ in vitro. ^{35}S-labelled $Cdc25B^{DAA}$ was efficiently ubiquitylated by SCF containing βTrCP1 or βTrCP2, in a JNK-dependent manner. By contrast, no ubiquitylated signal was detected when Skp2 or Cdc4 was used as the F-box protein (Fig. 2A). Furthermore, $βTrCP1^{ΔF}$ did not ubiquitylate Cdc25B (Fig. 2B). Note that $SCF^{βTrCP1}$ and $SCF^{βTrCP2}$ could ubiquitylate $Cdc25B^{DAA}$ without JNK, but JNK clearly enhanced the ubiquitylation (Fig. 2A,B). A high level of ubiquitylation was observed in the absence of JNK when wild-type Cdc25B was used for the in vitro ubiquitylation assay (Fig. 2C). Nevertheless, slight enhancement of Cdc25B ubiquitylation by $SCF^{βTrCP1}$ was observed in the presence of JNK activity (Fig. 2C). These results indicate that $SCF^{βTrCP}$ binds and ubiquitylates Cdc25B in a JNK-dependent manner, which is independent of the DDG constitutive binding site, and that a new JNK-regulated βTrCP-binding site is located in the N-terminal 175 amino acids of Cdc25B.

Our previous investigation suggested that S101 and S103 were possible target sites of JNK or p38 (Uchida et al., 2009). Therefore, we assessed the contributions of S101 and S103 to $SCF^{βTrCP}$-mediated $Cdc25B^{DAA}$ ubiquitylation. As indicated in Fig. 2D, whereas the ubiquitylation of Cdc25B was greatly compromised by S101A or S103A mutations, it was almost completely abolished with a S101A, S103A double mutant. These results indicate that the effects of S101 and S103 on Cdc25B ubiquitylation were collaborative. Other Cdc25B proteins, such as human Cdc25B3 and mouse Cdc25B1, were also ubiquitylated by $SCF^{βTrCP1}$ in the presence of JNK1 (supplementary material Fig. S1A). Intriguingly, $Cdc25B^{D94A}$ was hardly ubiquitylated (supplementary material Fig. S1A), suggesting that D94 in DAG is involved in JNK-induced Cdc25B ubiquitylation. Moreover, in such wild-type or mutant Cdc25B, βTrCP1 binding to Cdc25B proteins were roughly proportional to their ubiquitylation level (supplementary material Fig. S1B). Collectively, these results clearly indicate that JNK-induced Cdc25B degradation is mediated by $SCF^{βTrCP1}$, and that the phosphorylation of Cdc25B S101 and S103 plays an important role in this process.

JNK-induced Cdc25B degradation is aborted by βTrCP depletion

Next, we assessed the effects of βTrCP depletion on JNK-induced Cdc25B degradation using siRNA that targets both βTrCP1 and βTrCP2. We used either one siRNA, used in previous investigations

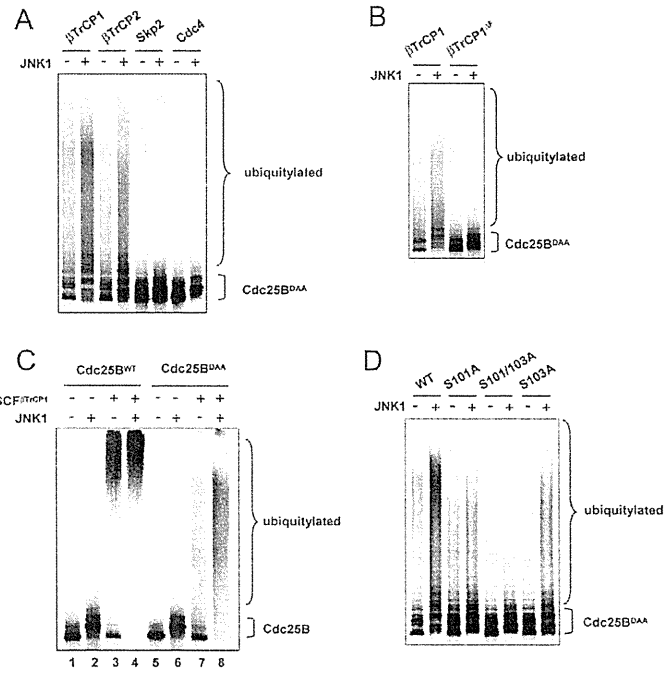

Fig. 2. Cdc25B is ubiquitylated by $SCF^{βTrCP}$ in vitro.
(**A**) [^{35}S]methionine-labelled $Cdc25B^{DAA}$ was incubated with each SCF complex in the presence or absence of JNK1, and ubiquitylation was determined as described in the Materials and Methods.
(**B**) [^{35}S]methionine-labelled $Cdc25B^{DAA}$ was incubated with each $SCF^{βTrCP1}$ or $SCF^{ΔβTrCP1}$ complex in the presence or absence of JNK1, and ubiquitylation was determined as described in A. (**C**) $SCF^{βTrCP1}$-mediated ubiquitylation of [^{35}S]methionine-labelled $Cdc25B^{WT}$ (wild type) or $Cdc25B^{DAA}$ was determined as described in A.
(**D**) [^{35}S]methionine-labelled $Cdc25B^{DAA}$ S101 and S103 (wild type), or with a mutation of S101A, S103A, or S101A and S103A (S101/103A), was incubated with $SCF^{βTrCP1}$ to determine ubiquitylation as described in A.

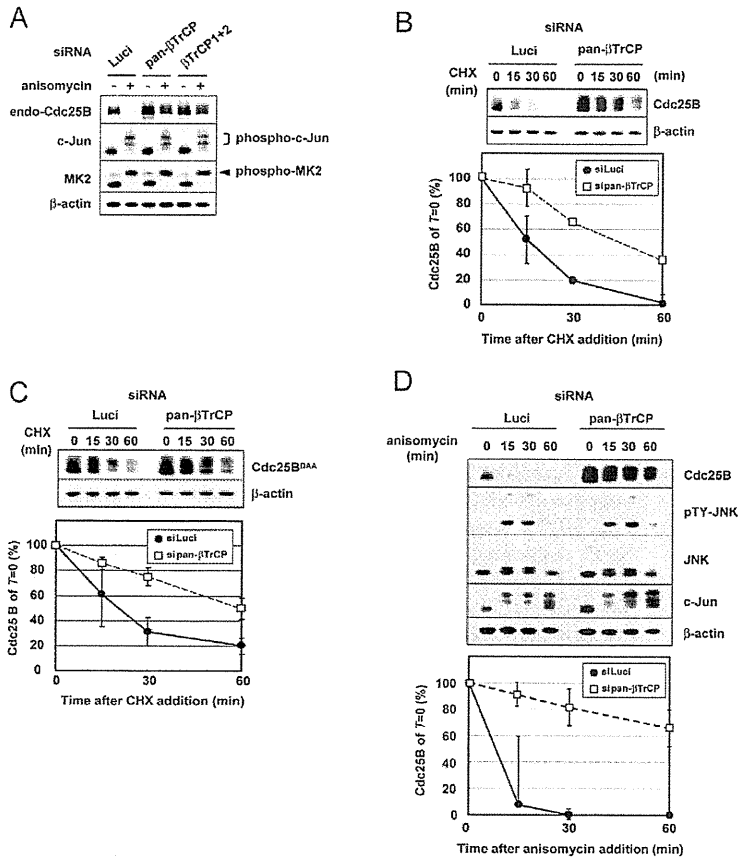

Fig. 3. βTrCP1 and 2 depletion stabilises Cdc25B. (**A**) HeLa cells were depleted of both βTrCP1 and 2 with siRNA (either pan-βTrCP or combined siRNA for βTrCP1 and 2). Luci indicates siRNA against luciferase, used as a control. After 24 hours, HeLa cells were treated with 50 ng/ml anisomycin for 30 minutes. The expression of endogenous Cdc25B was also determined by immunoprecipitation followed by immunoblotting. The expression of the other indicated proteins (Jun, MK2 and β-actin) was also determined by immunoblotting. (**B**) HeLa-W40 cells transfected with siRNA for either Luci or pan-βTrCP were treated with cycloheximide (CHX; 50 μg/ml), and expression of the indicated proteins was determined by immunoblotting at the indicated times. The relative Cdc25B expression is shown in the lower panel with the value at time 0 set at 100. The bars indicate the standard deviation (s.d.) of three independent experiments. (**C**) The expression of Cdc25B^{DAA} in HeLa-DAA34 cells in the presence of CHX was determined as described in B. (**D**) HeLa-W40 cells transfected with siRNA for either for Luci or pan-βTrCP were treated with 50 ng/ml anisomycin, and the expression of the indicated proteins was determined as described in B.

(Margottin-Goguet et al., 2003; Guardavaccaro et al., 2003) (denoted here as pan-βTrCP) or two in combination, which enabled us to knockdown either βTrCP1 or βTrCP2 specifically (denoted as βTrCP1 and 2). The effect on βTrCP depletion on introducing these siRNAs to HeLa-W40 cells that stably express FLAG–Cdc25B (Uchida et al., 2009) is shown in supplementary material Fig. S2A (we show only the expression of βTrCP1 because we had no specific antibody to βTrCP2). The results also indicated that the application of such siRNA to HeLa-W40 cells enhanced the expression of FLAG–Cdc25B and endogenous Cdc25A, suggesting that both Cdc25A and Cdc25B are destroyed via a βTrCP-mediated pathway, even in the absence of cellular stress (supplementary material Fig. S2A).

First, we examined the stability of endogenous Cdc25B after siRNA depletion of βTrCP1 and 2 with either siRNA for pan-βTrCP or combined siRNA for βTrCP1 and 2. As shown in Fig. 3A, βTrCP depletion substantially increased the resistance of endogenous Cdc25B under anisomycin stress. Moreover, transiently expressed Cdc25B^{DAA} also became refractory to the JNK-induced degradation on βTrCP1 and 2 depletion (supplementary material Fig. S2B). Because the depletion of βTrCP1 and 2 with the two siRNA treatments gave similar results (Fig. 3A and supplementary material Fig. S2A), we mainly used pan-βTrCP siRNA in the subsequent experiments.

Next, we asked whether the half-life of Cdc25B was affected by βTrCP depletion. HeLa-W40 cells stably expressing FLAG–Cdc25B were depleted of βTrCP1 and 2 with pan-βTrCP siRNA and the expression of Cdc25B protein was determined in the presence of cycloheximide. As indicated in Fig. 3B, wild-type Cdc25B appeared to be stabilised in βTrCP-depleted cells. Interestingly, the steady-state expression of constitutively expressed Cdc25B^{DAA} in HeLa-DAA34 cells was also less affected in βTrCP-depleted cells (Fig. 3C), suggesting that the SCF$^{\beta TrCP}$-mediated ubiquitin–proteasome pathway controls Cdc25B stability in unstressed conditions, through a site other than the DDG βTrCP-binding site.

We further investigated the involvement of βTrCP in anisomycin-induced Cdc25B degradation. FLAG–Cdc25B^{WT}-expressing HeLa-W40 cells were transfected with either luciferase or pan-βTrCP siRNA, followed by a 50 ng/ml anisomycin challenge. βTrCP1 and 2 depletion strongly compromised anisomycin-induced Cdc25B degradation (Fig. 3D). βTrCP depletion of FLAG–Cdc25B^{DAA}-expressing HeLa-DAA34 cells had similar effects (supplementary material Fig. S2B). Collectively, these results unequivocally indicate that SCF$^{\beta TrCP}$ directly controls the non-genotoxic stress-induced instability of Cdc25B. Furthermore, these results also suggest that a site other than the constitutive binding site DDG controls the steady-state stability of Cdc25B.

JNK phosphorylates Cdc25B under stressful conditions

Next, we investigated whether JNK or p38 phosphorylated S101 and S103 by raising antibodies that recognised S101-, S103- or S101 and S103-phosphorylated Cdc25B; the antibody specificity is shown in supplementary material Fig. S3A. Using these

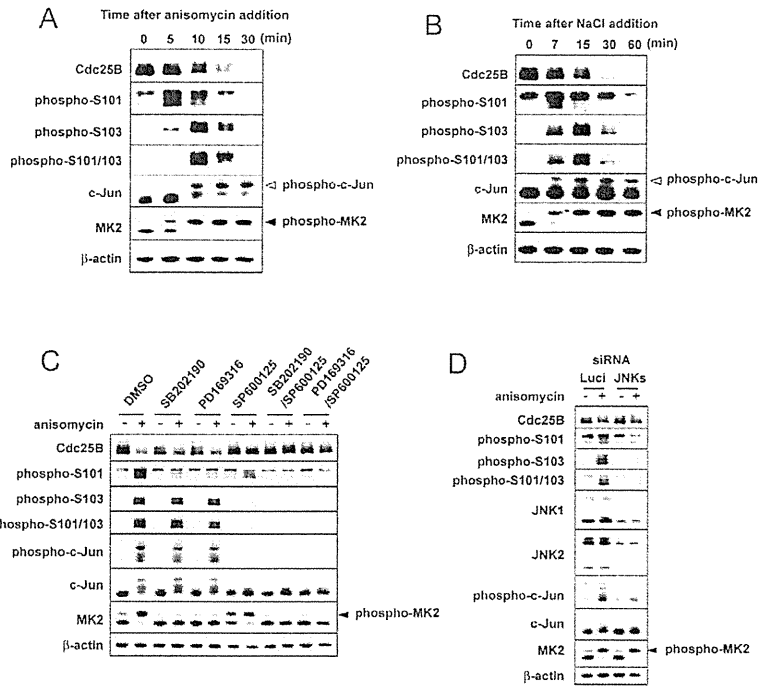

Fig. 4. Cdc25B S101 and S103 are phosphorylated by non-genotoxic insults. (**A**) HeLa-W40 cells that expressed FLAG–Cdc25B were treated with 50 ng/ml anisomycin. At the indicated times Cdc25B was immunoprecipitated, and phosphorylation was detected with antibodies. The expression of FLAG–Cdc25B, Jun, MK2 and β-actin are also shown. (**B**) HeLa-W40 cells were treated with 300 mM NaCl, and phosphorylation at S101 and S103 and the expression of the indicated proteins was detected, as described in A. (**C**) HeLa-W40 cells were treated with each inhibitor (5 μM each of SB202190 and PD169316 for p38 and 20 μM SP600125 for JNK, or a combination of SB and SP or PD and SP to inhibit p38 and JNK) 1 hour before the 50 ng/ml anisomycin challenge. Cell extracts were prepared after 10 minutes, and Cdc25B was immunoprecipitated. Phosphorylation at S101 and S103 and the expression of the indicated proteins were determined by immunoblotting. (**D**) HeLa-W40 cells were treated with siRNA for Luc or JNK (the siRNA for JNK was a mixture of one siJNK1 and two siJNK2). After 24 hours, the cells were treated with 50 ng/ml anisomycin for 10 minutes and cell extracts were prepared. The phosphorylation of Cdc25B at S101 and S103 and the expression of the indicated proteins were determined by immunoblotting.

antibodies, we investigated the phosphorylation status of S101 and S103 under either unstressed or stressed conditions. Conventional HeLa cells were not useful in these experiments because we could not recover enough Cdc25B by immunoprecipitation to detect its phosphorylation. We therefore used HeLa-W40 cells for phosphorylation analyses. Although a slight, but obvious, phosphorylated S101 (S101-*P*) signal was detected under unstressed conditions, S101 phosphorylation increased dramatically within 5 minutes of the 50 ng/ml anisomycin treatment, concomitant with p38 activation, as determined by the appearance of the phosphorylated form of MK2 (Fig. 4A). Unlike S101, the S103 phosphorylation signal was undetectable at time 0. A slight increase in phosphorylation was detected at 5 minutes and a much stronger signal was detected at 10 minutes, at which point JNK was fully activated, as determined by the Jun-*P* signal. The results for S103-*P* were similar to those for S101 and S103 double phosphorylation, for which the maximum level was detected at 10 minutes. Cdc25B phosphorylation decreased at 15 minutes and disappeared completely thereafter as a result of Cdc25B degradation. Similar results were obtained when stress was induced with 300 mM NaCl (Fig. 4B) or ultraviolet (UV) irradiation (supplementary material Fig. S3B). The steady-state phosphorylation of S101 and the similarity in the pattern between S103-*P* and the double S101-*P* and S103-*P* suggest that the phosphorylation of S103 occurs in S101-phosphorylated Cdc25B, because S101 is always phosphorylated in the absence of stress.

Next, we investigated the effects of the p38 inhibitors SB202190 and PD169316 (abbreviated to SB and PD, respectively) or the JNK inhibitors SP600125 (abbreviated to SP) on Cdc25B phosphorylation in HeLa-W40 cells. First, we determined suitable concentrations of these inhibitors for the specific inhibition of the respective kinases, because these kinases are often cross-inhibited by such inhibitors. As shown in supplementary material Fig. S4A, 20 μM SB inhibited both p38 and JNK activity, as determined by the disappearance of the phosphorylated MK2 and phosphorylated Jun signals, respectively, and it specifically inhibited p38 at a concentration as low as 5 μM without JNK inhibition. Supplementary material Fig. S4B,C also shows that 5 μM PD and 20 μM SP are suitable for the specific inhibition of p38 and JNK, respectively, without obvious cross-inhibition. As indicated in Fig. 4C, anisomycin-induced S101 phosphorylation was reduced by the p38 inhibitors SB and PD, but these inhibitors did not affect S103 phosphorylation. However, the JNK inhibitor SP completely inhibited S103, and modest inhibition of S101 phosphorylation was also observed. The role of JNK in S103 and S101 phosphorylation was also indicated by the siRNA depletion of JNK1 and JNK2 in anisomycin-treated HeLa-W40 cells, where the S101-*P* signal was reduced and the S101-*P*-103-*P* signal was almost completely abolished by the knockdown of both JNK1 and 2 (Fig. 4D). In a similar context, the clear reduction of the expression of endogenous Cdc25B by the transfection of wild-type, but not the kinase-dead mutant JNK1, also suggests that JNK functions in the degradation of endogenous Cdc25B (supplementary material Fig. S4D).

Collectively, these and our previous results indicate that the enhanced phosphorylation at S101 caused by p38 and JNK and de novo phosphorylation of S103 by JNK play crucial roles in stress-induced Cdc25B degradation. Furthermore, the S101-*P* signal detected under unstressed conditions did not disappear completely with the p38 inhibitors or JNK inhibitor, suggesting that an unidentified kinase(s) that phosphorylates S101 is involved in steady-state Cdc25B degradation.

The βTrCP-binding-motif-like DAG is essential for $SCF^{\beta TrCP}$-mediated Cdc25B ubiquitylation

The above results suggested that DAG, previously believed to be inactive, is functional in βTrCP-mediated Cdc25B ubiquitylation. To explore this possibility, we made a mutant Cdc25B in which

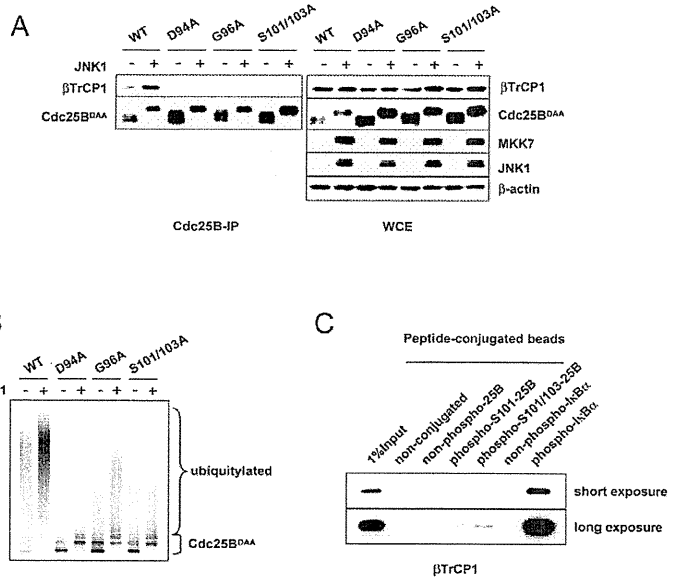

Fig. 5. Cdc25B peptide from D^{94}AG to S^{101}PSP is essential, but not sufficient, for Cdc25B ubiquitylation by SCF$^{\beta TrCP}$. (**A**) FLAG–Cdc25B of the wild type or indicated mutants was co-transfected with Myc–βTrCP1 in the presence or absence of JNK1. Then, 24 hours later, Cdc25B-bound βTrCP1 was detected by the immunoprecipitation of Cdc25B, followed by immunoblotting (Cdc25B-IP lanes). The expression of indicated proteins proteins is also shown (WCE lanes). (**B**) In vitro ubiquitylation by SCF$^{\beta TrCP1}$ of Cdc25B^{DAA} with wild-type DAG, or G96A or the double S101A, S103A mutations (S101/103A) was determined, as described in Fig. 2A. (**C**) Phosphorylated or unphosphorylated Cdc25B peptides, based on the sequence DAGLCMDSPSP that were conjugated with agarose beads, were incubated with Myc–βTrCP1-expressing Cos7 cell extracts and the βTrCP1 bound to peptides was detected by immunoblotting.

DAG was mutated to AAG (D94A), as the Asp in DSG plays a crucial role in substrate binding to βTrCP (Wu et al., 2003), and investigated whether the DAG in Cdc25B functions in JNK-induced βTrCP binding. FLAG–Cdc25B^{D94A} was co-transfected with βTrCP1 in the presence or absence of JNK1, and its binding to βTrCP1 was determined. Interestingly, Cdc25B^{D94A} failed to bind βTrCP1 (Fig. 4A). Cdc25B^{G96A} (DAA instead of DAG) was also unable to bind βTrCP1 (Fig. 4A). Furthermore, supplementary material Fig. S5A shows that both Cdc25B^{D94A} and Cdc25B^{G96A} were refractory to JNK-induced degradation (see also Fig. 1B). As expected, the Cdc25B S101A, S103A double mutant also lost βTrCP-binding ability. These results suggest that the Cdc25B peptide from D94 to S101 is a minimal requirement for βTrCP binding (see Fig. 1A). Moreover, the steady-state expression of such mutant Cdc25B was much higher than that of the wild-type protein (Fig. 5A). Therefore, the DAG sequence seems to be deeply involved in both the steady-state and stress-induced degradation of Cdc25B.

Next, we investigated how mutations in the DAG sequence affected in vitro Cdc25B ubiquitylation. Cdc25B^{D94A} was not ubiquitylated by SCF$^{\beta TrCP1}$, even in the presence of JNK activity; its ubiquitylation level was much less than that of the S101A, S103A double mutant (Fig. 5B). Cdc25B ubiquitylation was also greatly compromised by a G96A mutation, suggesting that G96 plays a role in Cdc25B binding to βTrCP. Cdc25B^{D94A} was phosphorylated at S101 and S103 when JNK1 was co-transfected (supplementary material Fig. S5B), showing that the phosphorylation of SPSP occurs irrespective of DAG. These results indicate that DAG in Cdc25B is necessary for ubiquitylation by SCF$^{\beta TrCP}$.

To elucidate whether a peptide encompassing DAG to SPSP was sufficient for βTrCP binding, we analysed βTrCP1 binding using the DAGLCMDSPSP peptide, in the unphosphorylated, S101-*P* and S101-*P*–P103-*P* forms. Peptide-conjugated beads were incubated with crude cell extracts prepared from βTrCP1-transfected Cos7 cells, and peptide-bound βTrCP1 was detected by immunoblotting. The unphosphorylated and phosphorylated IκBα peptides containing the conserved consensus βTrCP-binding sequence were used as controls. Fig. 5C shows that βTrCP1 barely bound the Cdc25B phospho-peptide under conditions where strong binding to the phosphorylated IκBα peptide was detected. Faint βTrCP1 signals that indicated binding to the doubly phosphorylated Cdc25B peptide were in fact detected by longer exposure. Taken together, these results strongly support the idea that DAG is a crucial sequence for JNK-induced Cdc25B ubiquitylation, but that the doubly phosphorylated DAGLCMDSPSP alone is insufficient for βTrCP binding.

The PEST-like sequence plays an important role in SCF$^{\beta TrCP}$-mediated Cdc25B ubiquitylation

Compared with Cdc25A, human Cdc25B possesses a longer PEST-like sequence that is rich in Glu (E) and Ser but lacks Pro (P), and is located upstream from DAG (Fig. 1A). This PEST-like sequence might contribute to βTrCP binding because phosphorylation or the presence of acidic amino acids N-terminal to the consensus DSG and DDG sequences facilitates βTrCP binding (Jin et al., 2003; Kanemori et al., 2005; Westbrook et al., 2008). The PEST-like sequence in Cdc25B comprises 12 amino acids, which consists of three ESS units and one LSS unit. We mutated all eight Ser to non-phosphorylatable Ala (S83A–S93A) and examined the binding of this sequence to βTrCP1. This Cdc25B^{8SA} mutant [denoted '8SA (–PEST)' in Fig. 5] was unable to bind βTrCP1 and was resistant to JNK-induced degradation (Fig. 6A and supplementary material Fig. S6A).

Next, we examined how many of the Cdc25B ESS–LSS sequences were necessary for βTrCP binding. We made a series of mutants with Ser-to-Ala mutations in the AA units, in which 2SA represents S83 and S84 to A, 4SA represents S83, S84, S86 and S87 to A, 6SA represents S86, S87, S89, S90, S92 and S93 to A, and 8SA is as described above (–PEST; see Fig. 6B) in the Cdc25^{DAA} background. The βTrCP-binding activity of these mutants was roughly proportional to the number of intact SS sequences (Fig. 6B). Consistent with these results, the degree of JNK-dependent ubiquitylation decreased in Cdc25B that lacked SS sequences (Fig. 6C). Cdc25B with fewer SS sequences was more refractory to JNK-induced degradation (supplementary

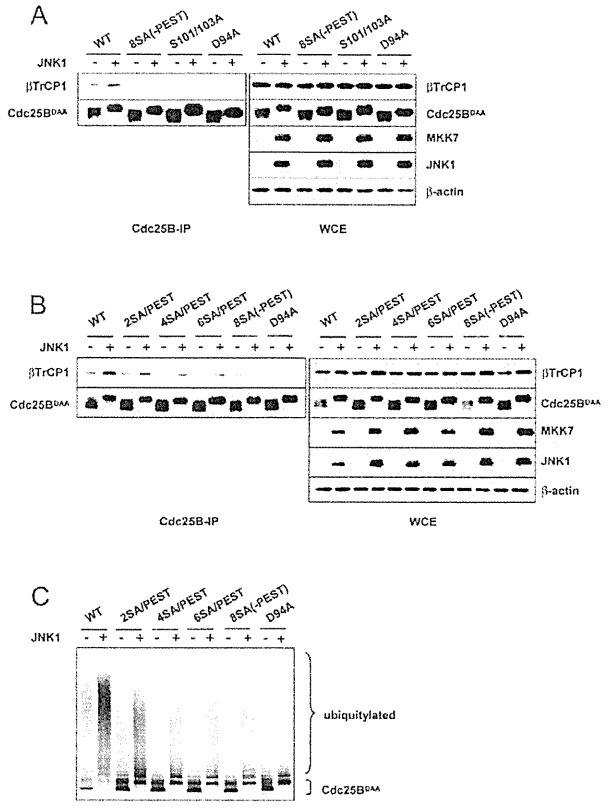

Fig. 6. The PEST-like sequence is required for efficient ubiquitylation of Cdc25B. (**A**) The following FLAG–Cdc25B^{DAA}-based mutants were co-transfected with Myc–βTrCP1 in the presence or absence of JNK1: WT with an intact PEST-like sequence; 8SA(–PEST) with mutations of eight Ser residues in the PEST-like sequence to alanine; the double S101A, S103A (S101/103A); or D94A. After 24 hours, Cdc25B was immunoprecipitated, and Cdc25B-bound βTrCP1 was detected by immunoblotting (Cdc25B-IP lanes). The expression of the indicated proteins was also determined (WCE lanes). (**B**) FLAG–Cdc25B^{DAA} with an intact PEST-like sequence (WT) or with SS to AA mutations of two Ser residues in three ESS units or one LSS unit was co-transfected with Myc–βTrCP1 in the presence or absence of JNK. The Cdc25B-bound βTrCP1 and protein expression are shown as indicated in A. Cdc25B^{D94A} was used as a negative control. (**C**) The ^{35}S-labelled Cdc25B^{DAA}-based proteins used in B were processed to detect in vitro ubiquitylation, as described in Fig. 2A.

material Fig. S6B). Of the four 2SA mutants (S83A and S84A, S86A and S87A, S89A and S90A, S92A and S93A), the mutant with SS mutations closest to DAG (S92A and S93A) was the most refractory to JNK-induced degradation and the least ubiquitylated, suggesting that ESS phosphorylation closer to DAG is more important for degradation (supplementary material Fig. S6C). The mutation in either E88 or E91 did not have any effect on JNK-induced degradation (supplementary material Fig. S6D), excluding the possibility that the PEST-like sequence itself is a core βTrCP-binding site. Moreover, S101 and S103 are phosphorylated in Cdc25B^{8SA}, indicating that the phosphorylation of S101 and S103 is independent of the PEST-like sequence (supplementary material Fig. S6E). Collectively, these results clearly indicate that a PEST-like sequence located upstream of DAG plays a crucial role in SCF^{βTrCP}-mediated Cdc25B ubiquitylation.

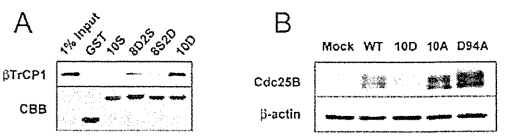

Fig. 7. A peptide encompassing the region between E^{82}SS and S^{101}PSP is a possible βTrCP-binding sequence in Cdc25B. (**A**) GST-fused Cdc25B-derived peptides consisting of the sequence E82SS to S101PSP were mixed with crude cell extracts prepared from Myc-tagged βTrCP1-transfected Cos7 cells, and this was followed by the recovery of proteins bound to GST-fused peptides. The recovered βTrCP1 was detected with anti-Myc antibody. The reaction mixture included 1 μM staurosporine to avoid the phosphorylation of Ser residues in the peptides by kinases present in the cell extracts. (**B**) FLAG–Cdc25B of wild type, 10D (all Ser residues in E^{82}SS to S^{101}PSP were replaced with Asp), 10A (all Ser residues in E^{82}SS to S^{101}PSP were replaced with Ala) or D94A were transfected into HeLa cells and their expression was determined by immunoblotting.

A stretch of PEST-like sequence up to S^{101}PSP of Cdc25B is a possible minimum sequence required for JNK-induced βTrCP binding

Next, we investigated the requirement of the PEST-like sequence and S^{101}PSP in βTrCP binding. Given the difficulty synthesising Ser-rich peptides and their phosphorylated forms, we made GST-fused peptides running from E^{82}SS to S^{101}PSP and their phospho-mimetic mutants, purified them from *Escherichia coli*, and investigated their binding to βTrCP1. The GST-fused peptides used were as follows: 10S (non-phosphorylated form), 8D2S (S-to-D mutation in the PEST-like sequence), 8S2D (D^{101}PDP mutant) and 10D (all S to D; Fig. 7A). Such *E. coli*-produced proteins were mixed with Myc–βTrCP1-expressing Cos7 cell extracts in the presence of 1 μM staurosporine to avoid phosphorylation of the GST-fused peptides by the kinases in Cos7 cell extracts. Peptide-bound βTrCP1 was detected by immunoblotting. As expected, the βTrCP1 bound to the phospho-mimetic peptides, but not the unphosphorylated one (Fig. 7A). βTrCP1 bound strongly to GST–10D, and less strongly to GST–8D2S and GST–8S2D. No βTrCP1 binding was detected for the GST-10S peptide. These results strongly suggest that the phosphorylation of Ser residues is required in the βTrCP-binding peptide consisting of the sequence from E^{82}SS to S^{101}PSP.

Next, we examined the stability of the Cdc25B^{10D} mutant in HeLa cells. Cdc25B of wild type, 10D, 10A (all Ser residues in E^{82}SS to S^{101}PSP were replaced by non-phosphorylatable Ala), and D94A were transfected to HeLa cells and their expression was detected in the absence of stress. As indicated in Fig. 7B, the expression of the phospho-mimetic Cdc25B^{10D} mutant was less than that of the wild type, indicating that Cdc25B^{10D} is unstable, even under unstressed conditions, supporting the idea that full βTrCP binding requires phosphorylation.

Finally, we investigated the contribution of the DAG and DDG βTrCP-binding sites to Cdc25B stability in stressed and unstressed conditions. FLAG–Cdc25B of wild type, Cdc25B^{D94A}, Cdc25B^{DAA} or Cdc25B$^{D94A/DAA}$ was transfected to HeLa cells and its expression was determined by immunoblotting. Typical expression of such mutants under anisomycin stress is shown in Fig. 8A. βTrCP1 binding to the Cdc25B mutant in the presence of JNK activity is also shown in supplementary material Fig. S7. As expected, Cdc25B^{WT} and Cdc25B^{DAA} were susceptible to anisomycin treatment and Cdc25B^{D94A} was more refractory to it. The

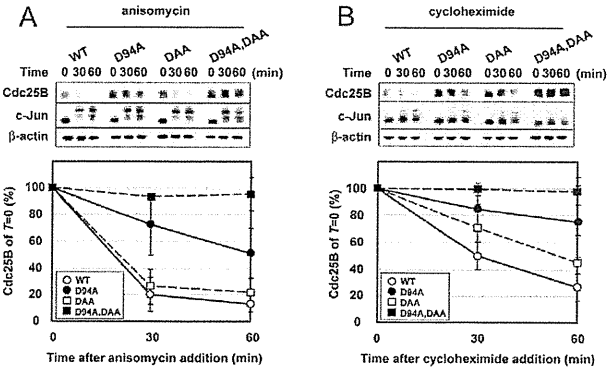

Fig. 8. DAG and DDG collaboratively regulate Cdc25B stability. FLAG-tagged Cdc25B^{WT}, Cdc25B^{D94A}, Cdc25B^{DAA} or Cdc25B$^{D94A/DAA}$ was transfected into HeLa cells, which were treated with 100 ng/ml anisomycin (**A**) or 50 μg/ml cycloheximide (**B**) 24 hours after transfection. Crude cell extracts were prepared at the indicated times and the expression of Cdc25B, Jun and β-actin was determined by immunoblotting. The relative expression of Cdc25B is also shown with the value at time 0 set to 100. The bars indicated the s.d. of five independent experiments. In A and B, the relative densitometric values of the expression of Cdc25B^{WT}, Cdc25B^{D94A}, Cdc25B^{DAA} and Cdc25B$^{D94A/DAA}$ were 1, 1.98±0.79, 1.77±0.59 and 4.21±1.2, respectively.

degradation of Cdc25B$^{D94A/DAA}$ was quite stable under anisomycin stress. These results indicate that the newly identified DAG βTrCP-binding sequence is responsible for stress-induced Cdc25B degradation. We also investigated the stability of such Cdc25B proteins in the presence of cycloheximide to estimate their steady-state stability (Fig. 8B). Cdc25B^{DAA} was more stable than Cdc25B^{WT}, but Cdc25B^{D94A} was even more stable than Cdc25B^{WT} or Cdc25B^{DAA}. Here again, the degradation of Cdc25B$^{D94A/DAA}$ was not observed with cycloheximide. These results suggest that the newly identified Cdc25B N-terminal βTrCP-binding region controls Cdc25B stability under both stressful and steady-state conditions and that the N-terminal DAG and constitutive DDG βTrCP binding sites cooperatively control Cdc25B stability.

Discussion

Previously, we showed that the cellular stresses that activate JNK or p38 induce Cdc25B degradation and that S101 and S103 are involved in Cdc25B stability (Uchida et al., 2009). We also suggested the involvement of the ubiquitin–proteasome system in stress-induced Cdc25B degradation. In this report, we identified SCF$^{\beta TrCP}$ as the ubiquitin ligase responsible for non-genotoxic stress-induced Cdc25B degradation. Moreover, S101 and S103 are highly phosphorylated by such stresses and are involved in ubiquitylation by SCF$^{\beta TrCP}$.

Our results indicate that non-canonical D^{94}AG and S^{101}PSP in Cdc25B play important roles in βTrCP binding. Moreover, an upstream PEST-like sequence starting from E^{82}SS turned out to have a crucial role in βTrCP binding to Cdc25B. Human Cdc25B has a longer PEST-like sequence than Cdc25A. The entire 12-amino-acid PEST-like sequence was essential for proper ubiquitylation. These results strongly indicate that the PEST-like sequence and SPSP cooperate with DAG for Cdc25B ubiquitylation under conditions that activate p38 and JNK. Moreover, the newly identified βTrCP-binding sequence around DAG is probably involved in Cdc25B degradation in collaboration with DDG under both stress-induced and steady-state conditions, given that the Cdc25B$^{D94A/DAA}$ double mutant was stable irrespective of cellular stress and SCF$^{\beta TrCP}$ barely ubiquitylated Cdc25B$^{D94A/DAA}$. Hence, we confidently conclude that Cdc25B stability is regulated mainly by SCF$^{\beta TrCP}$-mediated ubiquitylation via two independent sites: DAG and DAA.

The Ser residues in S^{101}PSP, located downstream from D94AG, are highly phosphorylated upon JNK and p38 activation. In addition, a GST-fused phospho-mimetic peptide consisting of E^{82}SS to S^{101}PSP bound βTrCP1, whereas that with the wild-type PEST-like sequence with SPSP did not, suggesting that the highly phosphorylated PEST-like sequence in Cdc25B is crucial for βTrCP binding. These results strongly suggest that full phosphorylation of the stretch from E^{82}SS to S^{101}PSP is required for Cdc25B to bind βTrCP. Such phosphorylation might confer a negative charge. The importance of phosphorylation in the upstream sequences to the core DSG sequence has also been reported in Cdc25A and REST (Jin et al., 2003; Westbrook et al., 2008). The stability of *Xenopus* Cdc25A was also found to be strongly affected by negatively charged amino acids surrounding the constitutive βTrCP-binding motif DDG (Kanemori et al., 2005). Hence, the βTrCP-binding-motif-like DAG sequence in Cdc25B functions in βTrCP binding by virtue of the strong negative charge resulting from acidic residues, which might enable a strong interaction with βTrCP. Analysis of the crystal structure should confirm this.

Under non-genotoxic stress, the Ser residues of the SPSP sequence are preferentially phosphorylated by p38 and JNK. Interestingly, S101 was weakly but constitutively phosphorylated under steady-state conditions when both p38 and JNK were inactive. These results indicate that an unidentified proline-directed kinase(s) phosphorylates S101 in the steady-state condition, which might contribute to Cdc25B degradation during the interphase. In this context, Isoda et al. reported the inhibition of phosphorylation by the CDK inhibitor p21 in the corresponding Ser residue in *Xenopus* Cdc25A (Isoda et al., 2009). Perhaps the interphase-specific CDK–cyclins that are active from the G1 phase to the S phase, such as Cdk2–cyclin E, Cdk2–cyclin A, and possibly Cdk4–cyclin D, phosphorylate S101 to keep Cdc25B expression low. The identification of a kinase that phosphorylates Cdc25B S101 under steady-state conditions is probably important for understanding the post-translational regulation of Cdc25B. A need for phosphorylation in the Cdc25B PEST-like sequence for βTrCP binding was also suggested. Given that the phosphorylation of Ser residues in the PEST-like sequence is a prerequisite for βTrCP binding, it is also important to identify the kinase(s) responsible for a full understanding of Cdc25B regulation. More work is needed to understand the regulation of Cdc25B stability by phosphorylation under steady-state and stress-induced conditions.

In conclusion, we identified a new site in Cdc25B for non-genotoxic stress-induced βTrCP binding and proved that SCF$^{\beta TrCP}$ is the responsible ubiquitin ligase. The newly identified site is DAG, which is thought to be inactive in βTrCP binding; it is surrounded by an upstream PEST-like sequence and a downstream SPSP. Our results suggest that the full phosphorylation of the PEST-like sequence and SPSP are required for βTrCP binding and that the new site and the previously reported DDG constitutive βTrCP binding site collaboratively regulate the stability of Cdc25B under both stress-induced and steady-state conditions. Cdc25B and Cdc25A are overexpressed in many tumours, and their overexpression is correlated with a poor prognosis (Kristjansdottir and Rudolph, 2004; Boutros et al., 2007). The uncontrolled

expression of Cdc25B is itself toxic, as it induces premature entry into M phase (Karlsson et al., 1999) and possibly genomic instability. Further studies that elucidate the regulation of Cdc25B stability should increase our understanding of the role of Cdc25B in cell cycle control and the contribution of the deregulation of Cdc25B stability to tumorigenesis.

Materials and Methods

Reagents and plasmids

Reagents of the highest grade were obtained from Wako (Osaka, Japan) or Sigma. The following siRNAs were purchased from Dharmacon: βTrCP1–βTrCP2 [denoted as pan-βTrCP siRNA in reports by Margottin-Goguet et al. and Guardavaccaro et al. (Margottin-Goguet et al., 2003; Guardavaccaro et al., 2003)], βTrCP1 (5′-UGACAA-CACUAUCAGAUUA-3′), and βTrCP2 (5′-GGACUUUAUUACCGCUUUA-3′). The validated stealth RNAi for JNK1 (5′-GGGCCUACAGAGAGCTAGUUCU-UAU-3′) and JNK2 (5′-GCCCAAGGGAUUGUUUGUGCUGCAU-3′ and 5′-GC-CAACUGUGAGGAAUUAUGUCGAA-3′) were obtained from Invitrogen. The siRNA for luciferase (5′-CGUACGCGGAAUACUUCGA-3′) was obtained from Qiagen. Anisomycin, SB202190, PD169316 and SP600125 were obtained from Calbiochem. The following cDNAs were used: human Cdc25B1, human Cdc25B3, mouse Cdc25B1, mouse p38α, mouse MKK6, mouse JNK1, mouse MKK7, human βTrCP1, human βTrCP2, human Skp1, human Skp2, human Cdc4, human Cul1 and mouse Rbx1. FLAG-, HA- and Myc-tagged expression plasmids were constructed using the pEF6/Myc-His vector, which includes the EF1α promoter (Invitrogen), as described elsewhere (Uchida et al., 2004). The mutant versions of the above cDNAs were generated by PCR-based mutagenesis, and their nucleotide sequences were confirmed by sequencing.

Antibodies and proteins

Active JNK1 kinase was purchased from Invitrogen. The rabbit antibody specific for Cdc25B S101-*P* was obtained from GenScript Corporation using NH_2-MD-*P*SPSPMDPHMAEC-COOH as the antigen. The rabbit antibodies specific for S103-*P*, and S101-*P* and S103-*P* were obtained from IBL (Japan) using NH_2-MDSP-*P*SPMDPHMAEC-COOH and NH_2-MD-*P*SP-*P*SPMDPHMAEC-COOH as the respective antigens. Each anti-phosphorylated antibody was affinity purified with antigen peptide before use. The antibodies purchased were as follows: mouse anti-TrCP1 was purchased from Zymed; Cdc25A (F-6), Cdc25B (C-20) and JNK1 (C-17) antibodies were from Santa Cruz Biotechnology; anti-actin, Myc tag (9B11), HA tag 262K, phosphoylated JNK–T183/Y185 (G9), MK2, Jun and phosphorylated Jun-S63II were obtained from Cell Signaling. The anti-Cdc25B (AF1649) was obtained from R&D Systems. Secondary antibodies labelled with horseradish peroxidase were purchased from DAKO. Anti-FLAG–M2-agarose beads were purchased from Sigma. The rabbit anti-FLAG serum was raised in-house. *E. coli*-produced GST-fused Cdc25B peptides encompassing $E^{82}SS$ to $S^{101}PSP$ and the phospho-mimetic mutant versions were purified from IPTG-induced BL21 cells with glutathione beads (GE Healthcare).

Cells, cell culture and siRNA or plasmid transfection

HeLa and Cos7 cells were grown in Dulbecco's modified Eagle's medium (DMEM) containing high glucose (Sigma) supplemented with 10% foetal bovine serum (FBS; Hyclone) and antibiotics. HeLa-W40 cells that constitutively expressed FLAG-tagged wild-type Cdc25B under the EF1α promoter were also cultured under the same conditions (Uchida et al., 2009). We also isolated HeLa cells constitutively expressing the FLAG-tagged $Cdc25B^{DAA}$ mutant (HeLa-DAA34 cells). In these cells, the expression of external Cdc25B was roughly 20- to 40-fold higher than that of endogenous Cdc25B. Plasmids were transiently transfected with Lipofectamine 2000 (Invitrogen). The amount of plasmid DNA used for transfection was ~500 ng for a six-well plate. HeLa and Cos7 cells were used for assays of stability (degradation) and for protein–protein interaction, respectively. The siRNA was transfected using Lipofectamine RNAiMAX (Invitrogen).

Biochemical methods and in vitro ubiquitylation assay

Crude extraction of proteins for analysis followed by immunoblotting or immunoprecipitation was performed as described previously (Uchida et al., 2004). The in vitro ubiquitylation assay was performed essentially as described previously (Watanabe et al., 2004). Briefly, HA-tagged Rbx1, Skp2 and Cul1, and Myc-tagged F-box proteins were coexpressed in Cos7 cells, and the SCF complex was recovered by immunoprecipitation with anti-Myc–agarose (MBL, Japan). [^{35}S]methionine-labelled Cdc25B was prepared with a TNT-coupled transcription and translation system (Promega). The reaction mixture in a total volume of 20 μl contained SCF-complex on beads, ^{35}S-labelled Cdc25B (2 μl), 20 μg bovine ubiquitin (Sigma), 0.8 μg human recombinant E1 enzyme (BIOMOL), 1 μg human 6xHis–Ubc5 (Wako, Osaka, Japan) and an ATP-regenerating system (2 mM ATP, 10 mM creatine phosphate, 0.35 IU/ml creatine kinase, 0.6 IU/ml inorganic pyrophosphatase), supplemented with 5 μM MG132, 0.5 μM okadaic acid and 1 μM ubiquitin-aldehyde (Boston Biochem). When necessary, recombinant active JNK1 (25 ng) was added to the reaction. The mixtures were incubated at 37°C for 2 hours, followed by sodium dodecyl sulphate–polyacrylamide gel electrophoresis (SDS-PAGE) in a 2–15% gradient gel, and the ubiquitylated Cdc25B was visualised using the FUJI BAS system.

We thank S. I. Reed (Scripps Institute) for the generous gift of human Cdc4 plasmids. This work was supported by grants from the following institutions: The Ministry of Health, Labour and Welfare of Japan, the Ministry of Culture, Sports, Science and Technology of Japan, the Research Grants Council of Hong Kong, the Cosmetology Research Foundation, the Long-range Research Initiative (LRI) of the Japan Chemical Industry Association, and the Japan Science and Technology Agency.

Supplementary material available online at
http://jcs.biologists.org/cgi/content/full/124/15/2816/DC1

References

Baldin, V., Cans, C., Superti-Furga, G. and Ducommun, B. (1997). Alternative splicing of the human CDC25B tyrosine phosphatase. Possible implications for growth control? *Oncogene* **14**, 2485-2495.

Bartek, J., Lukas, C. and Lukas, J. (2004). Checking on DNA damage in S phase. *Nat. Rev. Mol. Cell Biol.* **5**, 792-804.

Boutros, R., Dozier, C. and Ducommun, B. (2006). The when and wheres of CDC25 phosphatases. *Curr. Opin. Cell Biol.* **18**, 185-191.

Boutros, R., Lobjois, V. and Ducommun, B. (2007). CDC25 phosphatases in cancer cells: key players? Good targets? *Nat. Rev. Cancer* **7**, 495-507.

Busino, L., Donzelli, M., Chiesa, M., Guardavaccaro, D., Ganoth, D., Dorrello, N. V., Hershko, A., Pagano, M. and Draetta, G. F. (2003). Degradation of Cdc25A by beta-TrCP during S phase and in response to DNA damage. *Nature* **426**, 87-91.

Busino, L., Chiesa, M., Draetta, G. F. and Donzelli, M. (2004). Cdc25A phosphatase: combinatorial phosphorylation, ubiquitylation and proteolysis. *Oncogene* **23**, 2050-2056.

Chen, M. S., Hurov, J., White, L. S., Woodford-Thomas, T. and Piwnica-Worms, H. (2001). Absence of apparent phenotype in mice lacking Cdc25C protein phosphatase. *Mol. Cell. Biol.* **21**, 3853-3861.

Donzelli, M. and Draetta, G. F. (2003). Regulating mammalian checkpoints through Cdc25 inactivation. *EMBO Rep.* **4**, 671-677.

Ferguson, A. M., White, L. S., Donovan, P. J. and Piwnica-Worms, H. (2005). Normal cell cycle and checkpoint responses in mice and cells lacking Cdc25B and Cdc25C protein phosphatases. *Mol. Cell. Biol.* **25**, 2853-2860.

Frescas, D. and Pagano, M. (2008). Deregulated proteolysis by the F-box proteins SKP2 and beta-TrCP: tipping the scales of cancer. *Nat. Rev. Cancer* **8**, 438-449.

Galaktionov, K., Lee, A. K., Eckstein, J., Draetta, G., Meckler, J., Loda, M. and Beach, D. (1995). CDC25 phosphatases as potential human oncogenes. *Science* **269**, 1575-1577.

Guardavaccaro, D., Kudo, Y., Boulaire, J., Barchi, M., Busino, L., Donzelli, M., Margottin-Goguet, F., Jackson, P. K., Yamasaki, L. and Pagano, M. (2003). Control of meiotic and mitotic progression by the F box protein beta-Trcp1 *in vivo*. *Dev. Cell* **4**, 799-812.

Isoda, M., Kanemori, Y., Nakajo, N., Uchida, S., Yamashita, K., Ueno, H. and Sagata, N. (2009). The extracellular signal-regulated kinase-mitogen-activated protein kinase pathway phosphorylates and targets Cdc25A for $SCF^{beta\text{-}TrCP}$-dependent degradation for cell cycle arrest. *Mol. Biol. Cell* **20**, 2186-2195.

Jin, J., Shirogane, T., Xu, L., Nalepa, G., Qin, J., Elledge, S. J. and Harper, J. W. (2003). $SCF^{beta\text{-}TrCP}$ links Chk1 signaling to degradation of the Cdc25A protein phosphatase. *Genes Dev.* **17**, 3062-3074.

Kakizuka, A., Sebastian, B., Borgmeyer, U., Hermans-Borgmeyer, I., Bolado, J., Hunter, T., Hoekstra, M. F. and Evans, R. M. (1992). A mouse cdc25 homolog is differentially and developmentally expressed. *Genes Dev.* **6**, 578-590.

Kanemori, Y., Uto, K. and Sagata, N. (2005). Beta-TrCP recognizes a previously undescribed nonphosphorylated destruction motif in Cdc25A and Cdc25B phosphatases. *Proc. Natl. Acad. Sci. USA* **102**, 6279-6284.

Karlsson, C., Katich, S., Hagting, A., Hoffmann, I. and Pines, J. (1999). Cdc25B and Cdc25C differ markedly in their properties as initiators of mitosis. *J. Cell Biol.* **146**, 573-584.

Kristjansdottir, K. and Rudolph, J. (2004). Cdc25 phosphatases and cancer. *Chem. Biol.* **11**, 1043-1051.

Latres, E., Chiaur, D. S. and Pagano, M. (1999). The human F box protein beta-TrCP associates with the Cul1/Skp1 complex and regulates the stability of beta-catenin. *Oncogene* **18**, 849-854.

Lee, G., White, L. S., Hurov, K. E., Stappenbeck, T. S. and Piwnica-Worms, H. (2009). Response of small intestinal epithelial cells to acute disruption of cell division through CDC25 deletion. *Proc. Natl. Acad. Sci. USA* **106**, 4701-4706.

Lincoln, A. J., Wickramasinghe, D., Stein, P., Schultz, R. M., Palko, M. E., De Miguel, M. P., Tessarollo, L. and Donovan, P. J. (2002). Cdc25b phosphatase is required for resumption of meiosis during oocyte maturation. *Nat. Genet.* **30**, 446-449.

Ma, Z. Q., Chua, S. S., DeMayo, F. J. and Tsai, S. Y. (1999). Induction of mammary gland hyperplasia in transgenic mice over-expressing human Cdc25B. *Oncogene* **18**, 4564-4576.

Margottin-Goguet, F., Hsu, J. Y., Loktev, A., Hsieh, H. M., Reimann, J. D. and Jackson, P. K. (2003). Prophase destruction of Emi1 by the $SCF^{betaTrCP/Slimb}$ ubiquitin